HARMONIC COILS

Animesh K. Jain

RHIC Project, Brookhaven National Laboratory, Upton, New York 11973-5000, USA

Abstract

The basic theory of radial and tangential coils for harmonic analysis is described. A 2m-pole harmonic coil is discussed as a special case. The expression for flux is generalized for a coil of arbitrary geometry. The effects of transverse and torsional vibrations in the rotational motion are derived, leading to the need for bucking. A generalized bucking algorithm is presented for measuring magnets of different multipolarities with a tangential coil design used at RHIC. Simple, analytical estimates are provided for the errors in harmonic measurements resulting from a variety of random and systematic errors in the construction of measuring coils. Estimates are also provided for errors resulting from imperfect placement of the coil in the magnet. Such errors include a radial offset, sag and tilt of the measuring coil axis relative to the magnet axis. A procedure is given for accurate calibration of the geometric parameters of a five-winding tangential coil.

1.   INTRODUCTION

The field in the aperture of a long, relatively straight accelerator magnet can be considered to be two dimensional for most practical purposes. Such a field is generally described in terms of a harmonic expansion, as discussed in detail in another chapter in these proceedings [1]. The *field quality* in accelerator magnets is expressed in terms of the magnitude of undesirable harmonic terms in this expansion. Rotating coils, in which a loop of wire is rotated in the aperture of the magnet, provide the most convenient means to accurately measure these harmonic terms. Since these coils are used for harmonic measurements, such rotating coils are also referred to as *harmonic coils*.

The radial and azimuthal components of a two dimensional field in a current free region can be written as:

$$B_r(r,\theta) = \sum_{n=1}^{\infty} C(n)\left(\frac{r}{R_{ref}}\right)^{n-1} \sin[n(\theta - \alpha_n)] \tag{1}$$

$$B_\theta(r,\theta) = \sum_{n=1}^{\infty} C(n)\left(\frac{r}{R_{ref}}\right)^{n-1} \cos[n(\theta - \alpha_n)] \tag{2}$$

where $C(n)$ and α_n are constants and R_{ref} is an arbitrary *reference radius*, typically chosen to be 50-70% of the magnet aperture. The corresponding Cartesian components are most

conveniently described in terms of a complex field, $\boldsymbol{B}(\boldsymbol{z})$, defined as a function of the complex variable, $\boldsymbol{z} = x + iy = r \cdot \exp(i\theta)$, as:

$$\boldsymbol{B}(\boldsymbol{z}) = B_y(x, y) + iB_x(x, y) = \sum_{n=1}^{\infty} \left[C(n) \exp(-in\alpha_n) \right] \left(\frac{\boldsymbol{z}}{R_{ref}} \right)^{n-1} \tag{3}$$

It should be noted that all complex quantities are denoted by a bold and italic font in this paper. The real and the imaginary parts of the expansion coefficients in Eq. (3) are the normal and skew components respectively of the $2n$-pole term. In view of the different notations for the normal and skew components currently in use, we shall refrain from explicitly using these components. Accordingly, all equations in this chapter are written in terms of the parameters $C(n)$ and α_n. The two dimensional field is completely characterized in the aperture of the magnet by a set of the field parameters $C(n)$ and α_n (or equivalently, the normal and the skew components). The purpose of harmonic coils is to measure these field parameters in a magnet.

The basic principle of a harmonic coil is very simple. As a loop of wire is rotated in the field, a voltage signal is induced in the loop. The nature of this signal provides information on the angular dependence of the field, and hence its harmonic components according to Eqs. (1) and (2). Based on the geometry of the loop, there are two main types of harmonic coils –*radial* coils and *tangential* coils. The fundamental equations governing the use of such coils are described in Secs. 2 and 3. Special coil geometries, designed to be sensitive to selected harmonics, are treated in Sec. 4. Subsequent sections deal with the effects of imperfections in the rotational motion, random and systematic errors in coil construction and errors in aligning the coil axis with the magnet axis during measurements. Much of the material presented here follows closely the treatment in references [2] and [3]. The subject of harmonic coils is also covered in detail in references [4] to [6].

2.   THE RADIAL COIL

A cross section of a radial coil is shown schematically in Fig. 1. A radial coil has a flat loop of wire whose plane coincides with a radial plane of the rotating cylinder. More specifically, the two sides of the loop and the rotation axis lie in the same plane. The two sides of the loop are located at radii R_1 and R_2, as shown in Fig. 1. Such a coil is typically constructed by winding the loop on a flat bobbin, and then sandwiching it between the two halves of the rotating cylinder [6,7]. A radial coil is sensitive to the azimuthal component of the field, B_θ, as shown in Fig. 1. The flux, $\Phi_{radial}(\theta)$, through the coil at any angular orientation, θ, can be obtained by integrating the B_θ component given by Eq. (2) over the region covered by the radial coil:

$$\Phi_{radial}(\theta) = NL \int_{R_1}^{R_2} B_\theta(r, \theta) \, dr = \sum_{n=1}^{\infty} \frac{NLR_{ref}}{n} \left[\left(\frac{R_2}{R_{ref}} \right)^n - \left(\frac{R_1}{R_{ref}} \right)^n \right] C(n) \cos(n\theta - n\alpha_n) \tag{4}$$

where N is the number of turns and L is the length of the coil along the magnet axis. The above derivation assumes that the two sides of the coil loop are located on the same side of the rotation axis, as shown in Fig. 1. If the two sides are located on opposite sides of the
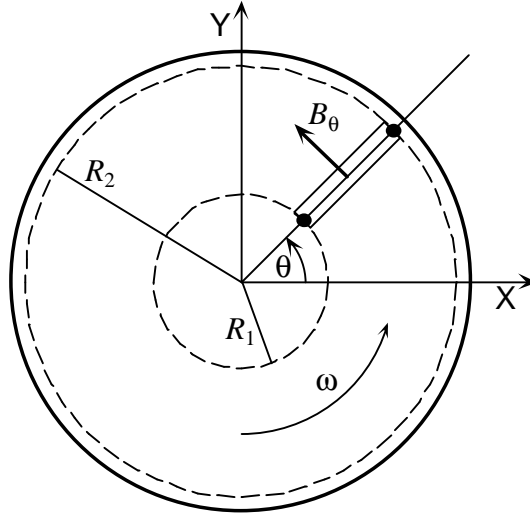
Fig. 1   Cross section of a radial coil.

rotation axis, as is true for many practical coils, then one should replace R_1 by $-R_1$. If the coil rotates with an angular velocity ω and $\theta = \delta$ is the angular position at time $t = 0$, then the flux as a function of time is given by:

$$\Phi_{\text{radial}}(t) = \sum_{n=1}^{\infty} \frac{NLR_{ref}}{n}\left[\left(\frac{R_2}{R_{ref}}\right)^n - \left(\frac{\pm R_1}{R_{ref}}\right)^n\right]C(n)\cos(n\omega t + n\delta - n\alpha_n) \quad (5)$$

where the sign of R_1 depends on whether the rotation axis is outside the region of the coil or inside it. Assuming a constant angular rotation speed, ω, the voltage signal induced in a radial coil is given by:

$$V_{\text{radial}}(t) = -\left(\frac{\partial \Phi_{\text{radial}}}{\partial t}\right) = \sum_{n=1}^{\infty} NLR_{ref}\,\omega\left[\left(\frac{R_2}{R_{ref}}\right)^n - \left(\frac{\pm R_1}{R_{ref}}\right)^n\right]C(n)\sin(n\omega t + n\delta - n\alpha_n) \quad (6)$$

A Fourier analysis of the voltage signal can give the amplitude, $C(n)$, and phase, α_n, of the $2n$-pole component of the field, provided the geometric parameters of the coil are known. The amplitude of the voltage signal is proportional to the angular velocity. If the angular velocity fluctuates during the rotation, the signal will be distorted and will give rise to spurious harmonics. For analysis based on voltage signals, it is essential to control the angular velocity and make corrections for any speed fluctuations. One way to overcome the dependence on angular speed is to integrate the voltage signal to get a signal proportional to the flux, which is independent of the angular speed:

$$\int V_{\text{radial}}(t)\,dt \equiv -\Phi_{\text{radial}}(\theta) = -\sum_{n=1}^{\infty} \frac{NLR_{ref}}{n}\left[\left(\frac{R_2}{R_{ref}}\right)^n - \left(\frac{\pm R_1}{R_{ref}}\right)^n\right]C(n)\cos(n\theta - n\alpha_n) \quad (7)$$

In the above equation, we have ignored the constant of integration, since any constant term is of no significance from the point of view of a Fourier analysis. As the coil rotates, the voltage

signal is integrated using an integrator, which is reset at $\theta = 0$. The output of the integrator is read out at several angular positions during the rotation. Typically, 128 or 256 angular positions are used to carry out fast, accurate Fourier transforms to obtain harmonics of interest in accelerator physics ($n \leq 15$). A more detailed account of the techniques can be found in an earlier review of the subject [5].

3.   THE TANGENTIAL COIL

A cross section of a tangential coil is shown schematically in Fig. 2. A tangential coil also has a loop of wire, similar to the radial coil. However, the plane of this loop is arranged to be normal to the radial vector drawn from the rotation axis to the center of the coil, as shown in Fig. 2. The two sides of the loop are equidistant from the rotation axis, and are located at a radius of R_c. Such a coil is sensitive to the radial component, B_r, of the magnetic induction. The flux, $\Phi_{\text{tang.}}(\theta)$, through such a coil at any angular position, θ, is:

$$\Phi_{\text{tang.}}(\theta) = NL \int_{\theta-\Delta/2}^{\theta+\Delta/2} B_r(R_c,\theta) R_c \, d\theta = \sum_{n=1}^{\infty} \frac{2NLR_{ref}}{n}\left(\frac{R_c}{R_{ref}}\right)^n \sin\left(\frac{n\Delta}{2}\right) C(n)\sin(n\theta - n\alpha_n) \quad (8)$$

where N is the number of turns, L is the length of the coil along the magnet axis and Δ is the angle subtended by the coil at the rotation axis, commonly referred to as the *opening angle*. If the coil rotates with an angular velocity ω and $\theta = \delta$ is the angular position at time $t = 0$, then the flux as a function of time is given by:

$$\Phi_{\text{tang.}}(t) = \sum_{n=1}^{\infty} \frac{2NLR_{ref}}{n}\left(\frac{R_c}{R_{ref}}\right)^n \sin\left(\frac{n\Delta}{2}\right) C(n)\sin(n\omega t + n\delta - n\alpha_n) \qquad (9)$$

Assuming a constant angular rotation speed, ω, the voltage signal induced in a tangential coil is given by:

$$V_{\text{tang.}}(t) = -\left(\frac{\partial \Phi_{\text{tang.}}}{\partial t}\right) = -\sum_{n=1}^{\infty} 2NLR_{ref}\,\omega\left(\frac{R_c}{R_{ref}}\right)^n \sin\left(\frac{n\Delta}{2}\right) C(n)\cos(n\omega t + n\delta - n\alpha_n) \quad (10)$$

Similar to the case of the radial coil discussed in Sec. 2, a Fourier analysis of the voltage signal can give the amplitude, $C(n)$, and phase, α_n, of the $2n$-pole component of the field, provided the geometric parameters of the coil are known. The remarks made in Sec. 2 concerning the angular speed fluctuations are equally applicable to tangential coils. The integrated voltage signal is proportional to the flux, and is independent of the angular speed:

$$\int V_{\text{tang.}}(t)\,dt \equiv -\Phi_{\text{tang.}}(\theta) = -\sum_{n=1}^{\infty} \frac{2NLR_{ref}}{n}\left(\frac{R_c}{R_{ref}}\right)^n \sin\left(\frac{n\Delta}{2}\right) C(n)\sin(n\theta - n\alpha_n) \qquad (11)$$

The radius, R_c, of the coil should be maximized to get good signal strength for higher harmonics. The opening angle, Δ, should be large enough to give good signal and small
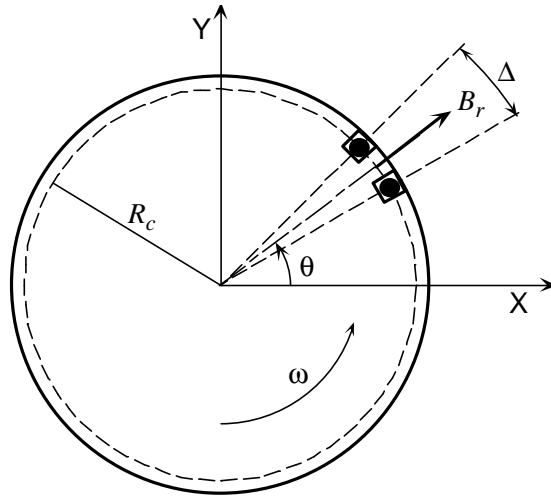
Fig. 2   Cross section of a tangential coil.

enough so that $\sin(n\Delta/2)$ does not vanish for higher harmonics of interest ($\Delta \ll 2\pi/n_{max}$). For most practical purposes, $\Delta \sim 15$ degrees can be considered optimum. A coil with an opening angle of only 10 degrees is more sensitive to harmonics higher than 28-pole as compared to a coil with an opening angle of 15 degrees, but at the expense of sensitivity for lower order terms. However, such high order multipoles are of limited interest for most accelerator physics studies. On the other hand, a coil with $\Delta = 20$ degrees is more sensitive than a coil with $\Delta = 15$ degrees for lower order harmonics, but the sensitivity begins to decline after only the 18-pole term.

4.   MULTIPOLE COILS

In general, the radial and the tangential coils described in the previous sections are sensitive to all harmonics. Sometimes, it may be advantageous to design a coil which is sensitive to only some multipoles. The most common examples of multipole coils are the dipole and the quadrupole coils used for *bucking* (see Sec.7).

4.1   A dipole coil

Let us first consider the special case of the simplest multipole coil— the dipole coil. A dipole coil has a flat loop of wire arranged in such a way that the rotation axis passes through the center of the loop, as shown in Fig. 3(a). Such a coil has a *Dipole Symmetry*, namely an antisymmetry under rotation by π radians. The flux through this coil can be calculated by treating it as a *radial coil* with $R_1 = -R_c$ and $R_2 = +R_c$, oriented at an angle θ, as illustrated in Fig. 3(a). The flux through the coil can also be calculated by treating it as a *tangential coil* with an opening angle of π radians, oriented at an angle of $\theta' = \theta + \pi/2$. Both approaches give the same expression for the flux:

$$\Phi_{\text{Dipole}}(\theta) = \sum_{\substack{n=1 \\ n=odd}}^{\infty} \frac{2NLR_{ref}}{n} \left(\frac{R_c}{R_{ref}} \right)^n C(n)\cos(n\theta - n\alpha_n) \tag{12}$$
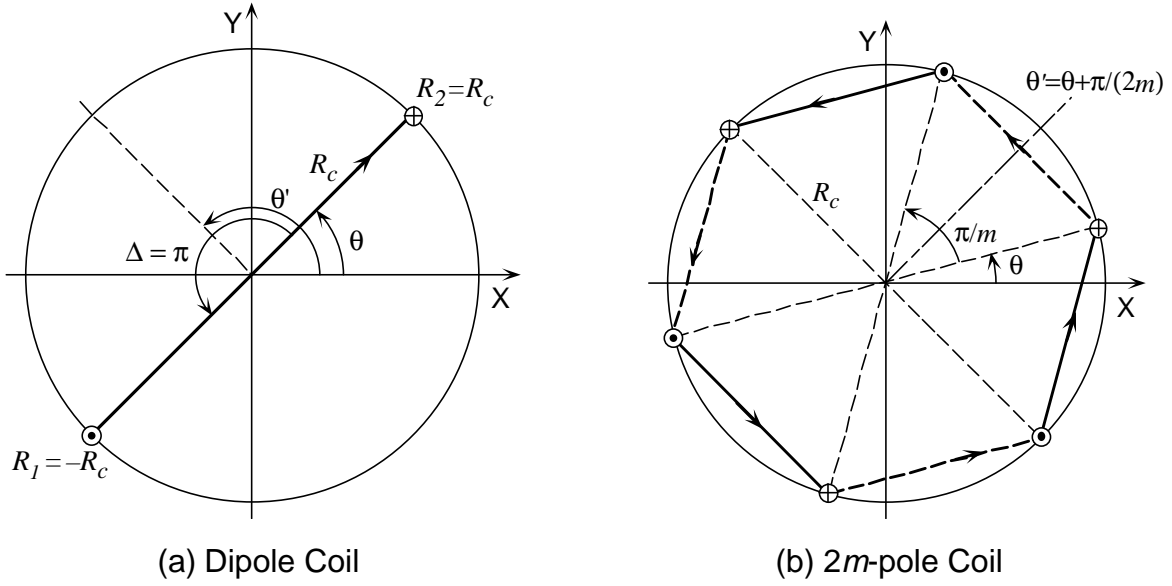
| (a) Dipole Coil | (b) 2*m*-pole Coil |

Fig. 3   (a) A dipole coil, which can be treated as either a radial, or a tangential coil and (b) A 2*m*-pole coil, which can be treated as *m* tangential coils in series, each with an opening angle of π/m and located every $2\pi/m$ radians.

It should be noted that the terms for even multipoles vanish in this particular geometry. A dipole coil is therefore sensitive to only the odd harmonics, i.e., dipole, sextupole, decapole, etc. Such a coil is almost universally used in both radial and tangential coil systems for bucking the main dipole field in a dipole magnet.

4.2   A multipole coil of order *m*

A multipole coil of order *m*, or a 2*m*-pole coil, is a generalization of the dipole coil described above. Such a coil, shown schematically in Fig. 3(b), has *m* loops connected in series. For any angular position characterized by the angle θ, the loops span the angular regions of θ to $\theta+(\pi/m)$, $(\theta+2\pi/m)$ to $(\theta+3\pi/m)$, $(\theta+4\pi/m)$ to $(\theta+5\pi/m)$, and so on. The flux through such a coil as a function of θ can be easily calculated by treating it as an array of *m* identical tangential coils with opening angle of $\Delta = \pi/m$ and having angular positions of $\theta' = \theta+(\pi/2m)$, $\theta' + 2\pi/m$, $\theta' + 4\pi/m$ and so on.

The flux through the first segment of the coil, covering the angular region θ to $\theta + \pi/m$, is:

$$\Phi_1(\theta) = \Phi_{\text{tang.}}(\theta') = \sum_{n=1}^{\infty} \frac{2NLR_{ref}}{n}\left(\frac{R_c}{R_{ref}}\right)^n \sin\left(\frac{n\pi}{2m}\right)C(n)\sin(n\theta' - n\alpha_n)$$

$$= \text{Im}\sum_{n=1}^{\infty} \frac{2NLR_{ref}}{n}\left(\frac{R_c}{R_{ref}}\right)^n \sin\left(\frac{n\pi}{2m}\right)C(n)\exp[i(n\theta' - n\alpha_n)]$$

(13)

The total flux through the array of loops is obtained by summing the contributions from all the segments located at angular intervals of $2\pi/m$:

$$\Phi_{2m\text{-pole}}(\theta) = \text{Im} \sum_{n=1}^{\infty} X_n \, e^{in\theta'} \left[1 + e^{i2\pi n/m} + e^{i4\pi n/m} + \ldots (m \text{ terms}) \right]$$

$$= \text{Im} \sum_{n=1}^{\infty} X_n \, e^{in\theta'} \left[\frac{1 - \exp(i2n\pi)}{1 - \exp(i2n\pi/m)} \right] \tag{14}$$

where,

$$X_n = \frac{2NLR_{ref}}{n} \left(\frac{R_c}{R_{ref}} \right)^n \sin\left(\frac{n\pi}{2m} \right) C(n) \exp(-in\alpha_n) \tag{15}$$

Since n is always an integer, the numerator of the quantity in square brackets in Eq. (14) is always zero. For integral values of (n/m), the denominator also vanishes and the quantity in square brackets has a limiting value of m. However, for even values of (n/m), the contribution again vanishes as the quantity X_n in Eq. (15) becomes zero due to the $\sin(n\pi/2m)$ factor. Therefore, all the harmonic terms in the summation vanish, except for those values of n which are odd multiples of m. For example, a quadrupole coil ($m = 2$) will only be sensitive to the quadrupole ($n = 2$), the dodecapole ($n = 6$), the 20-pole ($n = 10$), etc. terms. The total flux for the $2m$-pole coil can be written as:

$$\Phi_{2m\text{-pole}}(\theta) = \sum_{\substack{n=m \\ n=(2k+1)m}}^{\infty} \frac{2mNLR_{ref}}{n} \left(\frac{R_c}{R_{ref}} \right)^n C(n) \cos(n\theta - n\alpha_n) \tag{16}$$

where k is any integer, including zero. If the coil rotates with an angular velocity ω and $\theta = \delta$ is the initial angular position of the coil, then $\theta = \omega t + \delta$. The flux and the voltage at any time are given by:

$$\Phi_{2m\text{-pole}}(t) = \sum_{\substack{n=m \\ n=(2k+1)m}}^{\infty} \frac{2mNLR_{ref}}{n} \left(\frac{R_c}{R_{ref}} \right)^n C(n) \cos(n\omega t + n\delta - n\alpha_n) \tag{17}$$

$$V_{2m\text{-pole}}(t) = \sum_{\substack{n=m \\ n=(2k+1)m}}^{\infty} 2m\omega NLR_{ref} \left(\frac{R_c}{R_{ref}} \right)^n C(n) \sin(n\omega t + n\delta - n\alpha_n) \tag{18}$$

The results for a dipole coil are obtained by putting $m = 1$. Quadrupole coils ($m = 2$) are commonly used for bucking in tangential coil systems. Sextupole and other higher order coils may be used for special applications where it may be necessary to monitor or measure specific harmonics.

5. GENERAL TREATMENT OF ROTATING COILS

So far we have considered rotating coils of a specific geometry, such as the radial and the tangential coils. Even though the construction methods of these coils differ significantly due to the nature of their geometries, the underlying physics is quite similar for both types of coils. Consequently, it is advantageous to develop a formalism for a generalized coil shape. The radial and the tangential coils can then be treated as special cases of the general coil.

5.1 Flux through a coil of arbitrary shape

We consider a coil made up of a loop of wire running parallel to the Z-axis as shown in Fig. 4. The shape of the coil is defined by a path from the point z_1 to z_2 in the complex plane. The length of the loop is L along the *negative Z*-axis, as shown in Fig. 4.

Let $d\mathbf{r}$ be an element along the path from z_1 to z_2. The element of area, $d\mathbf{s}$, defined by this line element is given by

$$d\mathbf{s} = \hat{\mathbf{n}}|d\mathbf{r}|L = (\hat{\mathbf{z}} \times d\mathbf{r})L = \hat{\mathbf{z}} \times (\hat{\mathbf{x}}\,dx + \hat{\mathbf{y}}\,dy)L = (-dy\,\hat{\mathbf{x}} + dx\,\hat{\mathbf{y}})L \tag{19}$$

The flux through this area element $d\mathbf{s}$ is given by

$$d\Phi = \mathbf{B} \cdot d\mathbf{s} = (B_x\hat{\mathbf{x}} + B_y\hat{\mathbf{y}}).(-dy\hat{\mathbf{x}} + dx\hat{\mathbf{y}})L = (B_y\,dx - B_x\,dy)L = \text{Re}[\boldsymbol{B}(z)\,dz] \tag{20}$$

where $\boldsymbol{B}(z) = B_y + iB_x$ is the complex field defined in Eq. (3). This leads us to the general result for the flux through a loop with N turns:

$$\Phi = NL\,\text{Re}\left[\int_{z_1}^{z_2} \boldsymbol{B}(z)dz\right] = \text{Re}\left[\sum_{n=1}^{\infty} C(n)\exp(-in\alpha_n)\left(\frac{NLR_{ref}}{n}\right)\left\{\left(\frac{z_2}{R_{ref}}\right)^n - \left(\frac{z_1}{R_{ref}}\right)^n\right\}\right] \tag{21}$$
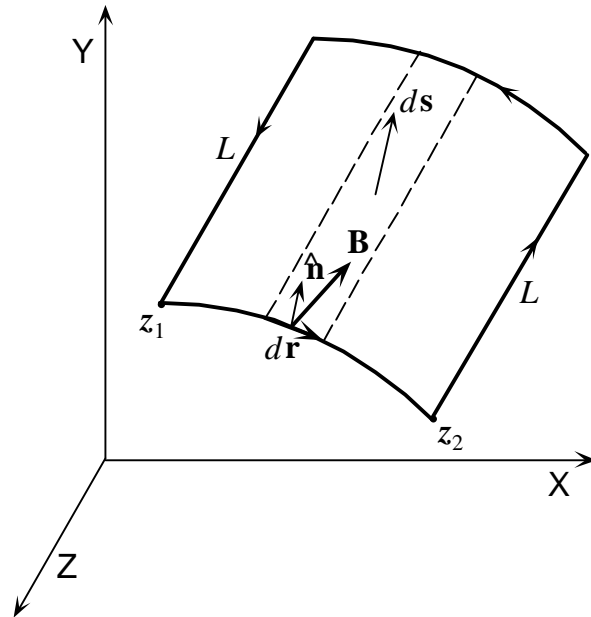

Fig. 4   Calculation of flux through a coil of arbitrary shape.

In writing Eq. (21), use has been made of the multipole expansion of the complex field, $\boldsymbol{B}(z)$, given by Eq. (3). For two-dimensional fields, the total flux depends only on the end points, z_1 and z_2, and not on the actual path followed by the loop between these points. This does not hold true for three dimensional fields in general, where $\boldsymbol{B}(z) = B_y + iB_x$ is no longer an analytic function of z.

5.2 A rotating coil of arbitrary shape

Let us consider a rotating coil of arbitrary shape formed by a loop of wire passing through two arbitrary points in the X-Y plane, as shown in Fig. 5. In general, both the radial and the azimuthal coordinates of these two points will be different. The *radial coil* is a special case where the *azimuthal* coordinates of both the points are either the same, or differ by π. Similarly, the *tangential coil* is a special case where the *radial* coordinates of the two points are the same. Any angular position of the coil is characterized by an angle θ measured from the "initial position" $(z_{1,0}, z_{2,0})$ of the wires. If z_1 and z_2 denote the locations of the two points in the complex plane at any instant, then the flux through the coil of length L and with N turns is given by Eq. (21). From Fig. 5,

$$z_1 = z_{1,0} \exp(i\theta); \quad z_2 = z_{2,0} \exp(i\theta) \tag{22}$$

Substituting in Eq. (21), we get,

$$\Phi(\theta) = \text{Re}\left[\sum_{n=1}^{\infty} \boldsymbol{K}_n \exp(in\theta) C(n) \exp(-in\alpha_n) \right] \tag{23}$$

where $\boldsymbol{K}_n$ is the *sensitivity factor* of the coil for the harmonic of order n and is given by:

$$\boldsymbol{K}_n = \left(\frac{NLR_{ref}}{n} \right) \left\{ \left(\frac{z_{2,0}}{R_{ref}} \right)^n - \left(\frac{z_{1,0}}{R_{ref}} \right)^n \right\} \tag{24}$$
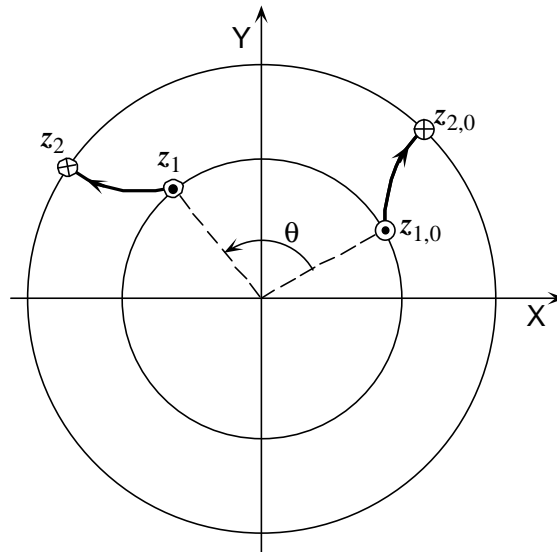

Fig. 5   A rotating coil of arbitrary shape

5.3 Radial and tangential coils as special cases

For a radial coil, when θ is measured from the X-axis, as shown in Fig. 1, $z_{1,0} = \pm R_1$ and $z_{2,0} = R_2$. It should be noted that $z_{1,0} = +R_1$ when R_1 and R_2 are on the same side of the center and $z_{1,0} = -R_1$ when R_1 and R_2 are on the opposite sides of the center. This gives,

$$K_n^{\text{radial}} = \frac{NLR_{ref}}{n}\left[\left(\frac{R_2}{R_{ref}}\right)^n - \left(\frac{\pm R_1}{R_{ref}}\right)^n\right] \tag{25}$$

The sensitivity factor for a radial coil is purely real in this case. Substituting in Eq. (23), we get the same expression for flux through a radial coil as was derived earlier in Eq. (4).

For a tangential coil, where θ denotes the angular position of the coil center measured from the X-axis (see Fig. 2), we have,

$$z_{1,0} = R_c \exp(i\Delta/2); \quad z_{2,0} = R_c \exp(-i\Delta/2) \tag{26}$$

$$K_n^{\text{tang.}} = -i\frac{2NLR_{ref}}{n}\left(\frac{R_c}{R_{ref}}\right)^n \sin\left(\frac{n\Delta}{2}\right) \tag{27}$$

The sensitivity factor for a tangential coil is purely imaginary. It can be easily verified that the expression for flux in Eq. (23) reduces in this case to that derived earlier in Eq. (8).

5.4 An array of rotating coils

Let us consider an array of M coils mounted on the same rotating system. Let the sensitivity factor of the j-th coil for the n-th harmonic be denoted by $K_n^{(j)}$, $j = 1,2,3,\cdots M$. Let all these coils be connected either in series, or in opposition, to generate a combined signal. The total flux through this array of coils is the algebraic sum of the fluxes through individual coils:

$$\Phi_{\text{Array}}(\theta) = \sum_{j=1}^{M} \beta_j \, \Phi_j(\theta) \tag{28}$$

where $\beta_j = +1$ if the j-th coil is connected in series, and $\beta_j = -1$ if the j-th coil is connected in opposition. In fact, one may consider a somewhat more general situation where the signals from the various coils are summed using a resistor/amplifier system. In this case, the flux corresponding to the resultant signal is still given by Eq. (28), where β_j are the appropriate amplification factors. From the general formula for the flux through an individual coil, we obtain:

$$\Phi_{\text{Array}}(\theta) = \sum_{j=1}^{M} \beta_j \left[\text{Re} \sum_{n=1}^{\infty} K_n^{(j)} \exp(in\theta) C(n) \exp(-in\alpha_n)\right] \tag{29}$$

If all the amplification factors, β_j, are purely real, then the expression for the total flux can be rearranged as:

$$\Phi_{\text{Array}}(\theta) = \sum_{j=1}^{M} \beta_j \left[\text{Re} \sum_{n=1}^{\infty} K_n^{(j)} C(n) \exp(-in\alpha_n) \exp(in\theta) \right]$$

$$= \text{Re} \sum_{n=1}^{\infty} \left(\sum_{j=1}^{M} \beta_j K_n^{(j)} \right) C(n) \exp(-in\alpha_n) \exp(in\theta) \qquad (30)$$

$$\equiv \text{Re} \sum_{n=1}^{\infty} K_n^{(\text{Array})} C(n) \exp(-in\alpha_n) \exp(in\theta)$$

From Eq. (30), the sensitivity factor of the overall array to the $2n$-pole term is:

$$K_n^{(\text{Array})} = \sum_{j=1}^{M} \beta_j K_n^{(j)}, \quad (\text{All } \beta_j \text{ must be real}) \qquad (31)$$

Thus, the overall sensitivity factor of the array is given by the algebraic sum of the sensitivities of individual coils in the array, provided the weight factors are purely real. In other words, any amplifier system used with the coil signals should not introduce a phase shift in the signals. If the individual coils are properly designed and β_j are appropriately chosen, the overall sensitivity of an array of coils to a particular harmonic (or a set of several harmonics) can be made zero. This is the principle used in the design of bucking windings discussed later in Sec. 7.

6.   IMPERFECTIONS IN COIL ROTATION: THE NEED FOR BUCKING

The expressions derived so far for the coil signals have assumed a perfect rotational motion. Such a perfect motion implies a rotation axis which is fixed and steady in space (no *transverse* vibrations), and no error in the angular positions at which the coil signals are to be sampled (no *torsional* vibrations). Since small amounts of such vibrations will invariably be present in any practical system, it is important to understand their effect on the measurement of harmonics. Typically, the undesired harmonics in an accelerator magnet are at the level of $\leq 10^{-4}$ of the fundamental field. Clearly, accurate measurement of these harmonics requires utmost care in eliminating the effects of imperfections in a practical system. It should be noted that while an irregular rotation speed is also an imperfection (and generally undesirable), one can, in principle, eliminate its effect either by integrating the voltage signal [see Eqs. (7) and (11)], or by measuring the instantaneous rotation speed and scaling the observed signal to a fixed rotation speed.

6.1   Transverse vibrations of the rotation axis

Let us consider a rotating coil of an arbitrary shape whose rotation axis has a displacement as the coil rotates. Such a transverse motion of the rotation axis is depicted schematically in Fig. 6. In the figure, the origin is assumed to be at the position of the rotation axis when the loop of the wire is at its *initial* location given by the points $(z_{1,0}, z_{2,0})$. The origin of the coordinate system is assumed fixed in space. As the coil rotates through an angle θ, the
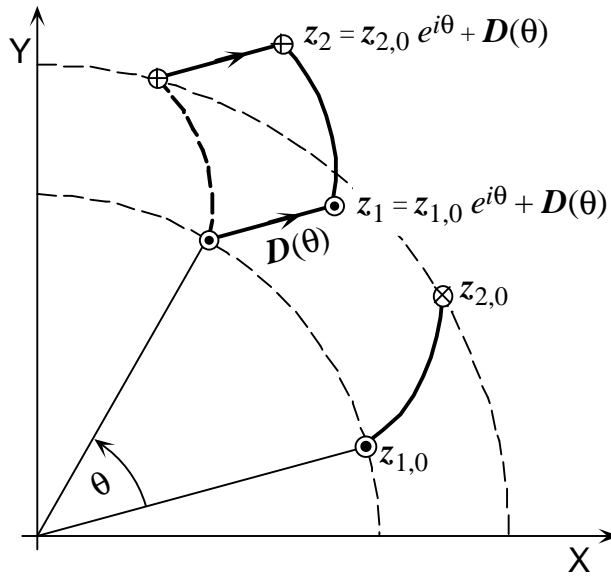
Fig. 6   Transverse vibrations of the rotation axis. As the coil rotates by an angle θ from the initial position given by $(z_{1,0}, z_{2,0})$, it gets displaced from the ideal position (shown by the thick dashed line) by $D(\theta)$.

axis of the coil undergoes a displacement $D(\theta)$ in the complex plane. Consequently, the positions of the two sides of the wire loop in the fixed coordinate system are given by

$$z_1 = z_{1,0} \exp(i\theta) + D(\theta); \quad z_2 = z_{2,0} \exp(i\theta) + D(\theta) \tag{32}$$

instead of the expressions in Eq. (22). The angular dependence of the flux through the coil can be obtained by substituting from Eq. (32) into Eq. (21). Let us examine the implications of the displacement $D(\theta)$ on the harmonic content of the measured flux through the coil. We shall assume that there is only one dominant harmonic in the magnetic field, as is indeed the case for most accelerator magnets.

6.1.1   A nearly pure dipole field

In a nearly pure dipole field, the expression for flux can be approximated by the $n = 1$ term in Eq. (21). The flux at any angular position, θ, is given by

$$\Phi(\theta) \approx \mathrm{Re}\left[NL\,C(1)\exp(-i\alpha_1)(z_2 - z_1) \right] = \mathrm{Re}\left[NL\,C(1)\exp(-i\alpha_1)\left(z_{2,0} - z_{1,0}\right)\exp(i\theta) \right] \tag{33}$$

The flux in this case depends only on the quantity $(z_2 - z_1)$, which is independent of the displacement, $D(\theta)$. Thus, the flux linked through a coil in a pure dipole field is unaffected by transverse displacements of the rotation axis. This result is not too surprising because a pure dipole field is uniform in space and displacements in such a field do not produce any feed down harmonics.

6.1.2   A nearly pure 2n-pole field

Let us now consider the measurement of harmonics in a nearly pure $2n$-pole field magnet ($n \geq 2$), such as a quadrupole, sextupole, etc. Once again, only one harmonic term in

the summation in Eq. (21) needs to be retained. An approximate expression for the flux in a pure $2n$-pole field can be obtained by using a binomial expansion and neglecting terms of the second and higher orders in $[\boldsymbol{D}(\theta)/R_{ref}]$, assuming that $|\boldsymbol{D}(\theta)| << R_{ref}$. We get:

$$\Phi_n(\theta) \approx \text{Re}\left[\boldsymbol{K}_n e^{in\theta} C(n)e^{-in\alpha_n}\right] + \text{Re}\left[\boldsymbol{K}_{n-1}e^{i(n-1)\theta}\left\{\frac{(n-1)\boldsymbol{D}(\theta)}{R_{ref}}\right\}C(n)e^{-in\alpha_n}\right] + \cdots \quad (34)$$

The first term in Eq. (34) represents the flux in the absence of a displacement. The flux picked up by a rotating coil in a pure $2n$-pole field is, in general, affected by transverse displacements of the rotation axis. To a first approximation, the effect is proportional to the amplitude of the displacement, $|\boldsymbol{D}(\theta)|$, and the sensitivity, $\boldsymbol{K}_{n-1}$, of the coil to the $2(n–1)$-pole term. It should be noted that the highest exponent of $\boldsymbol{D}(\theta)$ in the expression for the flux from a $2n$-pole field is $(n – 1)$. Thus, only the first term in the above expression survives for a pure dipole field, whereas the first two terms represent the complete expression for flux in a pure quadrupole field. For fields of higher multipolarities, other higher order terms are also present, but can be neglected since it is expected that the condition $|\boldsymbol{D}(\theta)| << R_{ref}$ will be satisfied for any decent measuring system.

The effect of transverse vibrations can be practically eliminated by making the sensitivity to the $2(n–1)$-pole term, $\boldsymbol{K}_{n-1}$, equal to zero when only the $2n$-pole term is the dominant term. *This is the basis for bucking the $2(n – 1)$-pole term in the measurement of a $2n$-pole magnet.* This *bucking* can be achieved, for example, by an array of coils. It should be noted that transverse vibrations make precise measurement of the $2(n–1)$-pole term difficult in a $2n$-pole magnet because the sensitivity, $\boldsymbol{K}_{n-1}$, can not be made zero. Such measurements are of interest, for example, in the determination of the magnetic axis. One must minimize the amplitude, $\boldsymbol{D}(\theta)$, of the transverse vibrations, or use a non-rotating coil system for this purpose.

6.1.3 Spurious harmonics due to periodic transverse motion

Let us assume that the displacement amplitude, $\boldsymbol{D}(\theta)$, is a periodic function of θ. This means that the coil follows the same motion in every rotation cycle. Such a periodic displacement may be expressed in terms of its Fourier components as,

$$\boldsymbol{D}(\theta) = \sum_{p=-\infty}^{\infty} \boldsymbol{D}_p \exp(ip\theta) \quad (35)$$

The expression for flux in a pure $2n$-pole field is given by Eq. (34). Substituting for $\boldsymbol{D}(\theta)$ from Eq. (35) into Eq. (34) and using the identity

$$\text{Re}\sum_{p=n}^{\infty} \boldsymbol{D}_{-p}e^{-i(p-n+1)\theta}\boldsymbol{K}_{n-1}C(n)e^{-in\alpha_n} = \text{Re}\sum_{p=n}^{\infty}\boldsymbol{D}_{-p}^*e^{i(p-n+1)\theta}\boldsymbol{K}_{n-1}^*C(n)e^{in\alpha_n} \quad (36)$$

the expression for flux in this case can be written as

$$\Phi_n(\theta) \approx \mathrm{Re}\left[\boldsymbol{K}_n e^{in\theta} C(n) e^{-in\alpha_n}\right] + \mathrm{Re}\left[\sum_{p=-n+2}^{\infty} \boldsymbol{K}_{n-1} e^{i(p+n-1)\theta} \frac{(n-1)\boldsymbol{D}_p}{R_{ref}} C(n) e^{-in\alpha_n}\right]$$

$$+ \mathrm{Re}\left[\boldsymbol{K}_{n-1} \frac{(n-1)\boldsymbol{D}_{-n+1}}{R_{ref}} C(n) e^{-in\alpha_n}\right] + \mathrm{Re}\left[\sum_{p=n}^{\infty} \boldsymbol{K}_{n-1}^* e^{i(p-n+1)\theta} \frac{(n-1)\boldsymbol{D}_{-p}^*}{R_{ref}} C(n) e^{in\alpha_n}\right]$$

(37)

The first term on the right hand side of Eq. (37) is the $2n$-pole term in the absence of vibrations. The other terms are spurious terms of other multipolarities. The amount of spurious $2m$-pole harmonic in the measured flux is given by:

$$C'(m) e^{-im\alpha'_m} \approx (n-1)\left[\left(\frac{\boldsymbol{K}_{n-1}}{\boldsymbol{K}_m}\right)\left(\frac{\boldsymbol{D}_{m-(n-1)}}{R_{ref}}\right)C(n)e^{-in\alpha_n} + \left(\frac{\boldsymbol{K}_{n-1}^*}{\boldsymbol{K}_m}\right)\left(\frac{\boldsymbol{D}_{-m-(n-1)}^*}{R_{ref}}\right)C(n)e^{in\alpha_n}\right] \quad (38)$$

For a pure $\sin(p\theta)$ displacement, only $\boldsymbol{D}_p$ and $\boldsymbol{D}_{-p}$ are non-zero. In a nearly pure $2n$-pole field, it follows from Eq. (38) that only the harmonics $m = (p+n-1)$, $(p-n+1)$, and $(n-p-1)$ are affected by such vibrations.

6.2 Torsional vibrations of the rotation axis

Let us now consider a type of rotational imperfection where the position of the rotating coil corresponding to angular position θ is not at θ, but at an angle of $\theta + T(\theta)$, as shown in Fig. 7. Such an imperfection may result either from an actual torsional vibration of the rotating coil, or it could be due to errors in the triggering of the data acquisition by the angle encoder. The position of the coil as a function of the angular parameter, θ, is given by:

$$z_1 = z_{1,0} \exp[i\theta + iT(\theta)]; \quad z_2 = z_{2,0} \exp[i\theta + iT(\theta)] \quad (39)$$
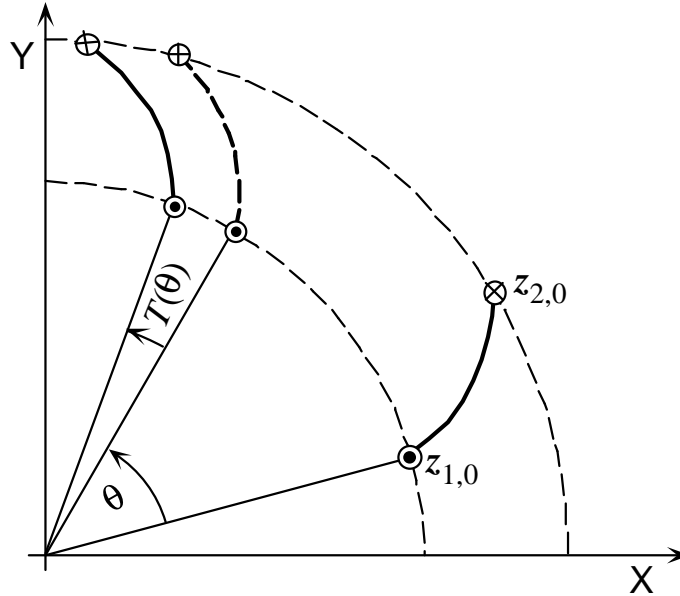

Fig. 7   Torsional vibrations of the rotation axis. As the coil supposedly rotates by an angle θ from the initial position given by $(z_{1,0}, z_{2,0})$, it is actually off from the ideal position (shown by the thick dashed line) by an angle $T(\theta)$.

6.2.1 Case of a nearly pure 2n-pole field

Substituting in the general expression for flux given by Eq. (21) and considering the case of small torsional amplitudes, we can write for the flux in a nearly pure 2n-pole field:

$$\Phi_n(\theta) \approx \mathrm{Re}\left[\boldsymbol{K}_n e^{in\theta}.C(n)e^{-in\alpha_n}\right] + \mathrm{Re}\left[in\boldsymbol{K}_n T(\theta)e^{in\theta}.C(n)e^{-in\alpha_n}\right] \tag{40}$$

The first term on the right hand side is the expected 2n-pole term in the absence of torsional vibrations. The second term will give rise to other spurious harmonics depending on the magnitude and angular dependence of $T(\theta)$. Terms of second and other higher orders in $T(\theta)$ are neglected in writing Eq. (40). To a good approximation, the amplitude of distortion in the flux seen by the coil is proportional to the amplitude of the torsional vibration as well as the sensitivity, $\boldsymbol{K}_n$, of the coil to the 2n-pole field. If the magnet has only one dominant harmonic, then the effect of torsional vibrations can be minimized by making the sensitivity of the coil (or an array of coils) zero for that particular harmonic. *This is the basis for bucking out the most dominant harmonic term from the pick up signal.* It should be noted that if the magnet has large allowed or unallowed multipoles, the effect of torsional vibrations is not completely cancelled by this bucking.

6.2.2 Spurious harmonics due to periodic torsional vibrations

Let us assume that the torsional vibration amplitude, $T(\theta)$, is a periodic function of θ. Such a periodic vibration can be expressed in terms of its Fourier components as

$$T(\theta) = \sum_{p=-\infty}^{\infty} \boldsymbol{T}_p \exp(ip\theta) \tag{41}$$

Substituting for $T(\theta)$ from Eq. (41) into Eq. (40) and using the identity

$$\mathrm{Re}\left[in\boldsymbol{T}_{-p}\boldsymbol{K}_n e^{-i(p-n)\theta}C(n)e^{-in\alpha_n}\right] = \mathrm{Re}\left[-in\boldsymbol{T}_{-p}^*\boldsymbol{K}_n^* e^{i(p-n)\theta}C(n)e^{in\alpha_n}\right] \tag{42}$$

the expression for flux in a nearly pure 2n-pole field can be written as

$$\begin{aligned}
\Phi_n(\theta) &\approx \mathrm{Re}\left[\boldsymbol{K}_n e^{in\theta}C(n)e^{-in\alpha_n}\right] + \mathrm{Re}\left[\sum_{p=-(n-1)}^{\infty} in\boldsymbol{T}_p\boldsymbol{K}_n e^{i(p+n)\theta}C(n)e^{-in\alpha_n}\right] \\
&+ \mathrm{Re}\left[in\boldsymbol{T}_{-n}\boldsymbol{K}_n C(n)e^{-in\alpha_n}\right] + \mathrm{Re}\left[\sum_{p=n+1}^{\infty} -in\boldsymbol{T}_{-p}^*\boldsymbol{K}_n^* e^{i(p-n)\theta}C(n)e^{in\alpha_n}\right]
\end{aligned} \tag{43}$$

The amount of spurious 2m-pole harmonics in the measured flux is given by:

$$C'(m)e^{-im\alpha'_m} \approx in\left[\left(\frac{\boldsymbol{K}_n}{\boldsymbol{K}_m}\right)\boldsymbol{T}_{m-n}C(n)e^{-in\alpha_n} - \left(\frac{\boldsymbol{K}_n^*}{\boldsymbol{K}_m}\right)\boldsymbol{T}_{-m-n}^*C(n)e^{in\alpha_n}\right] \tag{44}$$

If $T(\theta)$ has a simple angular dependence of the form $T_0\cos(p\theta)$ or $T_0\sin(p\theta)$ then only $\boldsymbol{T}_p$ and $\boldsymbol{T}_{-p}$ are non zero. We can see from Eq. (44) that such a motion will produce spurious harmonics corresponding to $2(n+p)$-pole and $2|(n–p)|$-pole field in a $2n$-pole magnet.

7.   IMPLEMENTATION OF BUCKING IN PRACTICAL COIL DESIGNS

It was shown in the previous section that existence of transverse and torsional vibrations in the rotational motion of a coil can produce spurious harmonics. To achieve a level of error at $\sim10^{-5}$ of the fundamental field, the tolerable amplitudes of such vibrations are impractically small. In other words, it is essential, in practice, to buck out at least the most dominant term and the next lower order feed down term in order to obtain accurate harmonics from the observed signal. This is usually achieved by an array of coils. Examples of such coils used in recent years are presented in this section. Since dipoles and quadrupoles are the most important magnets from the point of view of field quality in a high energy accelerator, most coil designs incorporate the ability to buck the dipole and the quadrupole components in a simple way. The same coils could also be used for measuring magnets of other multipolarities by incorporating signal amplifiers/attenuators or by using *digital bucking* (see Sec. 7.4)

7.1   Coils for HERA dipoles and quadrupoles

The magnets for the HERA accelerator at DESY were measured with radial coils [6]. For measuring dipole magnets, one needs to buck out only the dipole term. This can be achieved with a relatively simple design, as shown in Fig. 8(a), with only two windings. The outer winding (coil A) is the main winding and the central winding is used for bucking out the dipole term. In order to do this with a simple addition of the two signals, the following condition must be satisfied

$$N_A(r_2 - r_1) = N_B(r_3 + r_4) \tag{45}$$

where N_A and N_B are the number of turns in the two windings and the radii are as shown in Fig. 8(a). The two windings, A and B, had the same number of turns and the same width. In

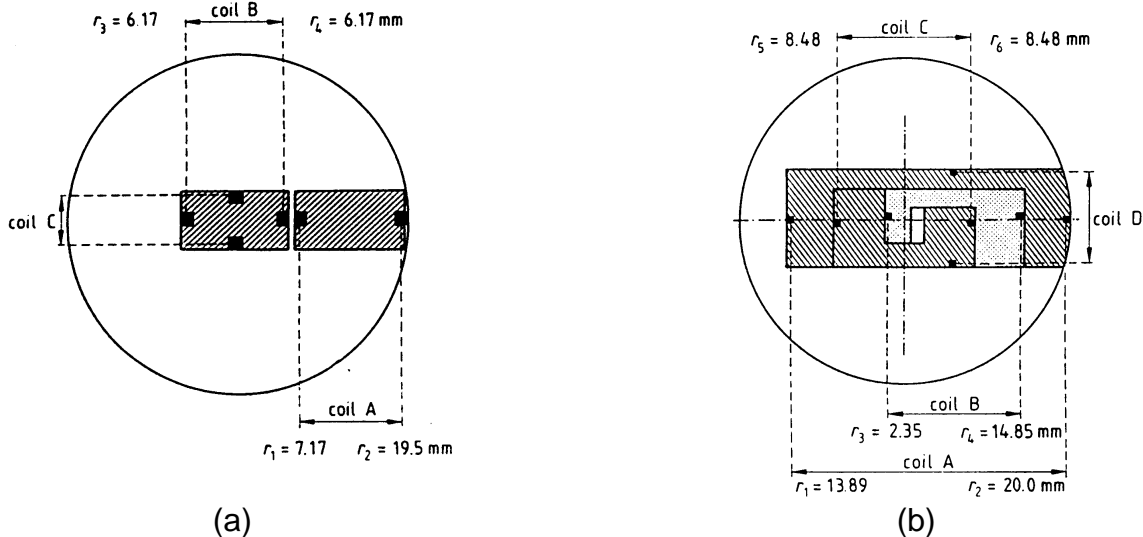(a)   (b)

Fig. 8   Design of radial coils used for measuring (a) the dipoles and (b) the quadrupole magnets for the HERA collider at DESY (from reference [6])

addition to satisfying Eq. (45) for matching the magnitude of the signals, it is also essential that the two windings be coplanar, so that the two signals have exactly the same (or opposite) phase. In practice, there may be an angular misalignment between the two windings due to construction errors. In order to correct for any resulting phase error, a third winding (coil C), orthogonal to the central winding, is also used.

In the case of the quadrupole magnets, one needs to buck out the quadrupole as well as the dipole terms. This requires a slightly more complicated geometry, as shown in Fig. 8(b). The system consists of three main coils, coils A-C, and a fourth coil (D) to compensate for any angular misalignments. Referring to Fig. 8(b), the conditions for bucking the dipole and the quadrupole components can be written as

$$N_A(r_2 + r_1) - N_B(r_3 + r_4) - N_C(r_5 + r_6) = 0 \tag{46}$$

$$N_A(r_2^2 - r_1^2) - N_B(r_4^2 - r_3^2) - N_C(r_6^2 - r_5^2) = 0 \tag{47}$$

where the bucked signal is given by

$$V_{\text{bucked}} = V_A - V_B - V_c \tag{48}$$

7.2   Tangential coils for the RHIC magnets

All magnets for the Relativistic Heavy Ion Collider (RHIC), currently nearing completion at the Brookhaven National Laboratory, are measured with a common tangential coil design [8,9] shown in Fig. 9. All windings are placed inside precisely machined grooves on the surface of an insulating cylinder. The system consists of a tangential winding (T1) with 30 turns and an opening angle of 15 degrees. A pair of dipole windings (D1 and D2) and a pair of quadrupole windings (Q1 and Q2) are used for bucking. The bucking windings have
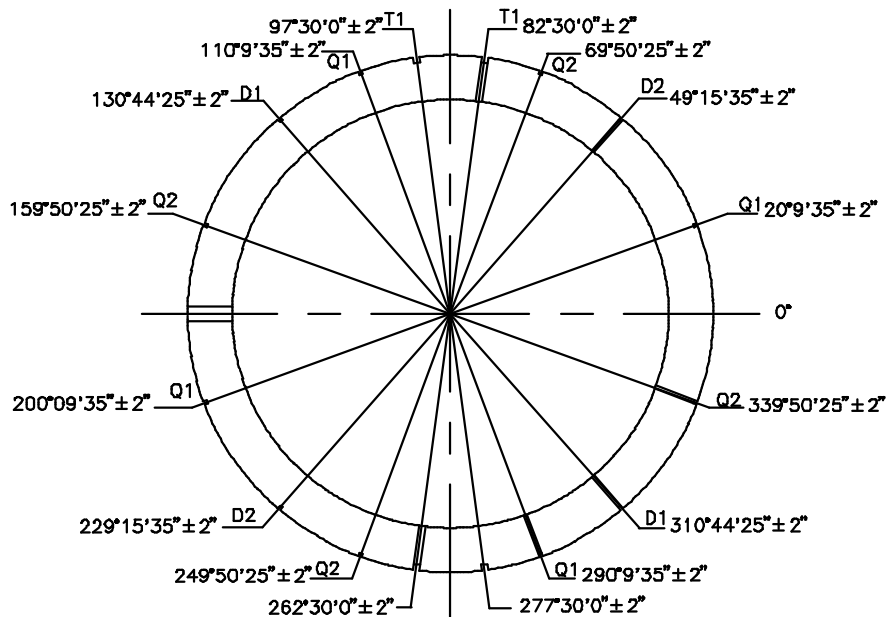

Fig. 9   A tangential coil design used to measure all the RHIC magnets. The pair of grooves opposite to the T1 winding are not used.

three turns each, and are of the type described in Sec. 4. The angular positions of the various bucking windings are chosen in such a way that a simple addition of all the five signals completely cancels the dipole and the quadrupole terms. While measuring dipole magnets with small harmonic content, it is essential only to buck the dipole term. The use of the quadrupole windings in this case is optional. Although the design of the coil system is common for all magnets, the outer radius of the cylinder on which the windings are placed is chosen to match the maximum available aperture in each magnet type. This provides the maximum accuracy in the measurement of higher harmonics specified at a reference radius which is approximately a fixed fraction (~ 0.625) of the magnet coil inner radius.

7.3   Measuring coils for the Large Hadron Collider (LHC)

At present, work is underway for construction of a Large Hadron Collider (LHC) at CERN. Several measuring coil systems have been designed [7,10] to measure various magnets in this accelerator. The radial coils to be used for measuring the dipole and the quadrupole magnets are shown in Figs. 10(a) and (b). The dipole radial coil, to be used for warm measurements, is a simple design with an external, main winding, and a central bucking winding. Both windings have 400 turns and are of the same width. The second external coil shown in Fig. 10(a) is mainly for mechanical symmetry, but it can also be used as a spare or for diagnostic purposes. The coils are fabricated very precisely and their alignment is very carefully controlled [7]. The phases of the two signals are therefore the same, making it unnecessary to use an orthogonal bucking winding. A simple addition (or subtraction) of the signals from the outer winding and the central winding results in a complete cancellation of the dipole term.

The radial coil system for measuring quadrupoles has five windings and is shown in Fig. 10(b). There is a pair of "outer" coils, a pair of "intermediate radius" coils, and a "central" coil. Only one of the "outer" coils is actually used in the harmonic measurements, while the other outer coil is a spare. The central coil is sensitive to the dipole term and insensitive to the quadrupole term. The two intermediate radius coils have equal and opposite sensitivities for the quadrupole term, but identical sensitivities for the dipole term. The outer coil is twice as sensitive as the intermediate radius coils for the quadrupole term. Thus, a
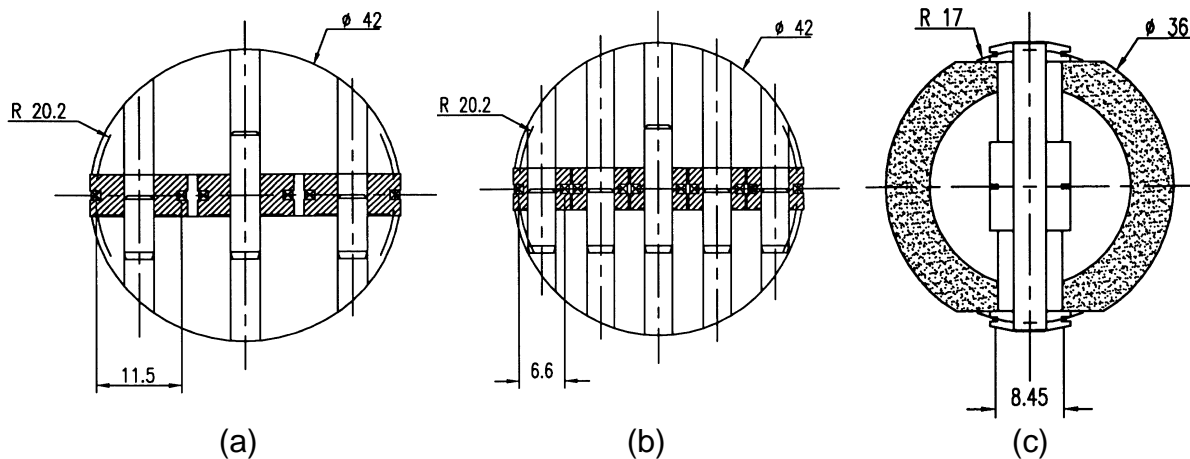

Fig. 10   Coil designs planned for measuring the magnets for LHC – (a) radial coil for dipoles, (b) radial coil for quadrupoles and (c) tangential coil for dipoles. [*Courtesy J. Billan, CERN*]

simple addition of the four signals with appropriate signs results in a cancellation of the dipole and the quadrupole terms. The same system can be used to buck out other harmonics when measuring magnets of a different multipolarity if the signals are added with weight factors other than ±1. This would normally require use of amplifiers with adjustable gains to suit magnets of different multipolarities.

For measurements of LHC dipoles in the superconducting state, it is planned to use a long chain of 13 simultaneously rotating coil assemblies to cover a length of 15 meters at the same time. Simultaneous coverage of the entire magnet is desirable due to time dependent effects in the superconductor. Each of these rotating coils consists of a tangential coil of 36 turns mounted on a ceramic form and a centrally located dipole bucking coil, as shown in Fig. 10(c). The tangential coil has a rather large opening angle of about 30 degrees for practical reasons, resulting in some loss of sensitivity for very high order harmonics. This is not expected to be a problem since this system will be used only for high field measurements, where the signals are sufficiently strong. The second tangential coil on the opposite side is for mechanical symmetry, but it can also be used as a spare or for diagnostic purposes.

7.4   Analog and digital bucking

In the preceding subsections, we have seen several examples of coil designs used for measuring dipoles and quadrupoles. A common feature of these designs is that all of them provide a cancellation of the dipole and the quadrupole terms with a simple addition of the signals. In practice, an exact cancellation of the signals is rarely achieved due to various construction errors. This necessitates either a resistor/amplifier network for precise compensation, or a very careful selection and adjustment of the coils to avoid significant construction errors. Implementation of bucking by actually combining the signals in this way is commonly referred to as *analog bucking*. Such a scheme is shown in Fig. 11. The most dominant component is obtained from the main winding directly, whereas all the other harmonic information is obtained from an analysis of the bucked signal. The analog bucking scheme has the advantage that it requires fewer data recording channels and a smaller dynamic range in the voltmeters or integrators. On the other hand, it is relatively difficult or cumbersome to change the weight factors of various signals in order to buck out different harmonics in magnets of different multipolarities.
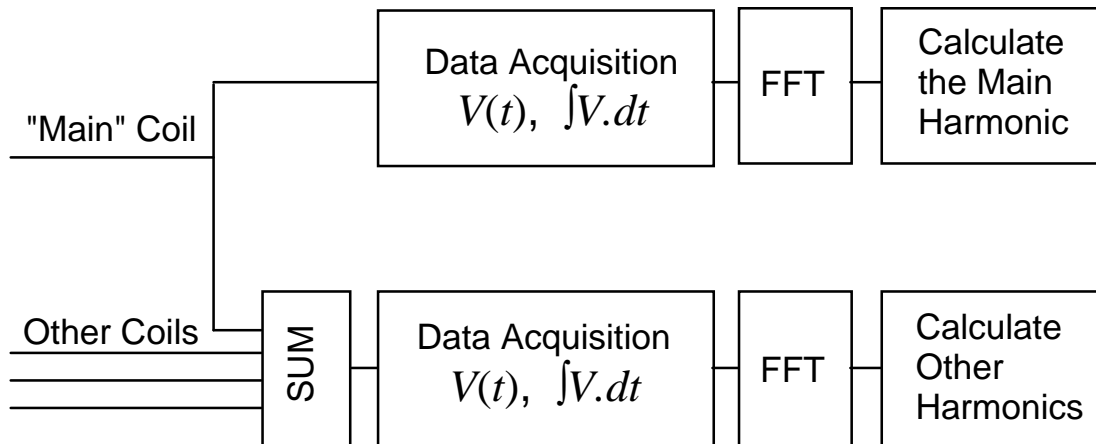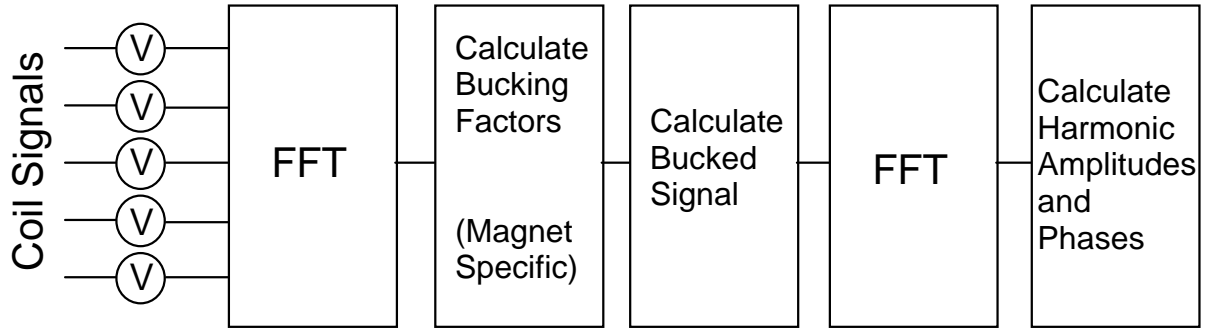

Fig. 11   Analog bucking scheme

Fig. 12　　Schematic of digital bucking.

The tangential coils are fabricated at Brookhaven National Laboratory (BNL) by winding the coils directly into grooves machined in the surface of an insulating cylinder. In this technique, it is not possible to produce a large number of coils, and then match those to the bucking coils. In order to accommodate reasonable construction errors and still achieve good bucking, a technique known as *digital bucking* has been used. In this technique, all the individual coil signals are recorded using digital voltmeters, as shown in Fig. 12. The bucked signal is generated digitally by adding the signals with appropriate weight factors in the analysis software. This technique allows one to use coils with significant construction errors (with proper calibration, of course). Also, the weight factors can be easily changed in the software to measure magnets of different multipolarities. A disadvantage of this method is that more recording channels are needed than in analog bucking, and the voltmeters must have good linearity over a large dynamic range.

The technique of digital bucking has been used successfully for measurement of the magnets for RHIC at BNL. An automated algorithm was developed that senses the multipolarity of the magnet being measured from a FFT of the tangential coil signal. The software then calculates the bucked signal, which is a superposition of signals from all the five windings (see Sec. 7.2 for the RHIC coil design) according to the relation

$$V_{\text{bucked}} = V_{\text{tangential}} + f_1 V_{\text{D1}} + f_2 V_{\text{D2}} + f_4 V_{\text{Q1}} + f_5 V_{\text{Q2}} \tag{49}$$

where the real coefficients f_1 to f_5 are calculated to buck out the most dominant, and the next lower order harmonic for any magnet. The dipole windings can be used to buck out the dipole, the sextupole, or the decapole term. The quadrupole windings can be used to buck out the quadrupole or the 12-pole terms. The RHIC coil design does not allow bucking of the octupole harmonic, since neither the dipole nor the quadrupole windings have any sensitivity for this term (see Sec. 4.2). If n_1 is the harmonic to be cancelled with the D1 and D2 windings, then the design values of f_1 and f_2 are given by:

$$f_1 = \left(\frac{N_3}{N_1}\right)\left(\frac{R_3}{R_1}\right)^{n_1} \frac{\sin\{n_1(\delta_3 - \delta_2)\}}{\sin\{n_1(\delta_2 - \delta_1)\}} \sin\left(\frac{n_1 \Delta}{2}\right) \sin\left(\frac{n_1 \pi}{2}\right)$$

$$f_2 = \left(\frac{N_3}{N_2}\right)\left(\frac{R_3}{R_2}\right)^{n_1} \frac{\sin\{n_1(\delta_1 - \delta_3)\}}{\sin\{n_1(\delta_2 - \delta_1)\}} \sin\left(\frac{n_1 \Delta}{2}\right) \sin\left(\frac{n_1 \pi}{2}\right)$$

$$\tag{50}$$

where the δ's are the angular positions of the windings at time $t = 0$. Similarly, if n_2 is the harmonic to be cancelled using the Q1 and Q2 windings:

$$f_4 = \left(\frac{N_3}{2N_4}\right)\left(\frac{R_3}{R_4}\right)^{n_2}\frac{\sin\{n_2(\delta_3 - \delta_5)\}}{\sin\{n_2(\delta_5 - \delta_4)\}}\sin\left(\frac{n_2\Delta}{2}\right)\sin\left(\frac{n_2\pi}{4}\right)$$

$$f_5 = \left(\frac{N_3}{2N_5}\right)\left(\frac{R_3}{R_5}\right)^{n_2}\frac{\sin\{n_2(\delta_4 - \delta_3)\}}{\sin\{n_2(\delta_5 - \delta_4)\}}\sin\left(\frac{n_2\Delta}{2}\right)\sin\left(\frac{n_2\pi}{4}\right)$$

(51)

The design values of these weight factors are given in Table 1 for various harmonics. In practice, these weight factors are determined from the FFT of the actual signals to account for any construction errors. As can be seen from the table, all the weight factors are unity for bucking the dipole and the quadrupole components. Thus, a properly built RHIC coil can also be used with analog bucking for dipoles and quadrupoles.

Table 1   Design values of weight factors to cancel various harmonics

n_1	f_1	f_2	n_2	f_4	f_5
1	−1.00	−1.00	2	−1.00	−1.00
3	−2.26	−2.26	6	−2.06	−2.06
5	+7.57	+7.57	—	—	—

8.   EFFECT OF COIL CONSTRUCTION ERRORS

So far, we have considered the effect of imperfections in the rotational motion of the coil, and the ways to overcome these effects using bucking. The measuring coil itself was assumed to be built perfectly as per design. In practice, a variety of systematic and random errors may be present due to limitations of the construction method. A systematic error, for example in the radius or the angular position of the coil, may not affect the measurements at all provided the error is accounted for in the analysis by a proper calibration. However, if one is using analog bucking, such systematic errors will result in poor bucking ratios, and are undesirable. In this section, we shall consider the effect of some of the coil construction errors on the measured harmonics.

8.1   Effect of a finite size of the coil windings

In practice, the coil windings are not point-like. To accommodate the necessary number of turns (which may be as high as several hundred), the winding must have a finite cross section. This could introduce errors in the measurement of the amplitudes of the harmonics, since different turns of the winding are at different radii.

Although a typical winding cross section is rectangular, it is convenient to approximate it with a sector of an annulus, as shown in Fig. 13(a). The winding is assumed to have an angular width of (2α) and thickness (2δ). The mean position of the winding is denoted by $z_0 = R.\exp(i\phi)$. The sensitivity factor of the winding to the $2n$-pole term [see Eq. (24)] involves the quantity z^n. The effective value of z^n averaged over the cross section of the winding can be obtained by integration as follows:

$$(z^n)_{avg.} = \frac{\int\limits_{R-\delta}^{R+\delta} r^n dr \int\limits_{\phi-\alpha}^{\phi+\alpha} \exp(in\phi)\,d\phi}{(2\alpha)(2\delta)} = \frac{\left[(R+\delta)^{n+1} - (R-\delta)^{n+1}\right]\left[e^{in(\phi+\alpha)} - e^{in(\phi-\alpha)}\right]}{4in(n+1)\alpha\delta}$$

$$= R^n \exp(in\phi)\frac{\sin(n\alpha)}{n\alpha}\frac{\left[\left(1+\dfrac{\delta}{R}\right)^{n+1} - \left(1-\dfrac{\delta}{R}\right)^{n+1}\right]}{2(n+1)(\delta/R)} \tag{52}$$

$$= z_0^n\,\frac{\sin(n\alpha)}{n\alpha}\frac{\left[\left(1+\dfrac{\delta}{R}\right)^{n+1} - \left(1-\dfrac{\delta}{R}\right)^{n+1}\right]}{2(n+1)(\delta/R)}$$

If the winding is assumed to be point like and located at the geometric center, z_0, the above formula gives the error in estimating the amplitude of the $2n$-pole term. Expanding in a power series, it can be shown that the leading correction terms are of the second order in α and (δ/R). In deriving the above formula, it has been assumed that the density of turns varies inversely with the radius. In other words, a layer of the winding at a larger radius has the same *number* of turns as a layer at a smaller radius. If one assumes a constant *density* of turns, then the layer at a larger radius will have a slightly higher number of turns. The quantity $(n+1)$ in the last factor on the right hand side of Eq. (52) should be replaced with $(n+2)$ in this case.

The calculated errors in the amplitudes of various harmonics are shown in Fig. 13(b) for windings of 1 mm × 1 mm cross section placed at mean radii of 10 mm and 25 mm. For the case of a 25 mm radius, the error is negligible for all harmonics of interest. The errors are more pronounced for a smaller radius coil. However, even for a 10 mm radius coil, the errors may not be serious since the higher harmonics in most accelerator magnets are very small, at the level of a *unit* (10^{-4} of the most dominant term) or less and a 1% error in their values is generally negligible. The finite size may, however, have a serious effect while measuring the
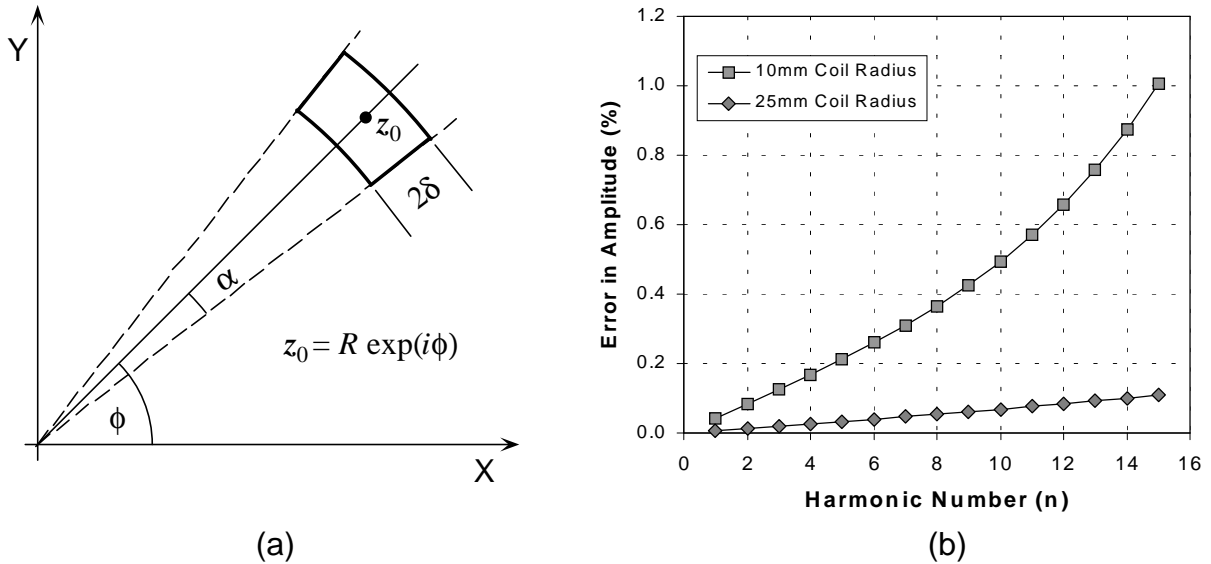

(a)   (b)

Fig. 13   (a) A coil winding of a finite size, and (b) errors in the amplitudes of various harmonics with a 1 mm × 1 mm winding for different coil radii. In calculating the errors, the winding is assumed to have a mean position z_0, as shown in (a).

transfer function of higher multipole magnets (such as sextupoles, octupoles, etc.) with a small diameter measuring coil. In such instances, it may be desirable to apply a correction to the observed amplitudes.

In calculating the errors shown in Fig. 13(b), it has been assumed that the effective radius of the winding is given by the geometric center, as shown in Fig. 13(a). It should be noted that Eq. (52) gives a correction factor equal to $\sin\alpha/\alpha$ even for the dipole term. This is because the geometric center is not the center of gravity in the case of a sector of an annulus. If the effective radius is taken to be $z_0(\sin\alpha/\alpha)$ instead of z_0, which is equivalent to determining the radius from a calibration in a reference dipole magnet, then the errors are considerably reduced from those given by Eq. (52). For a winding with the same width as height ($\alpha = \delta/R$), it can be shown in this case that the second order correction terms vanish, and the leading correction terms are of the fourth order in (δ/R).

In practice, the windings are generally of a rectangular shape, as shown in Fig. 14(a). It can be shown that for a rectangular winding of height h and width w, the average value of z^n is given by

$$(z^n)_{avg.} = z_0^n \cdot \left[\frac{\xi_1^{n+2} \sin\{(n+2)\lambda_1\} - \xi_2^{n+2} \sin\{(n+2)\lambda_2\}}{2(h/2R)(w/2R)(n+1)(n+2)} \right] \qquad (53)$$

where
$$\xi_{1,2} = \sqrt{\left(1 \pm \frac{h}{2R}\right)^2 + \left(\frac{w}{2R}\right)^2}; \quad \lambda_{1,2} = \tan^{-1}\left[\frac{(w/2R)}{1 \pm (h/2R)}\right] \qquad (54)$$

Fig. 14(b) shows the errors calculated for 1 mm^2 rectangular windings of 10 mm radius and different aspect ratios. It is seen that the errors are significantly smaller for a square shape ($w/h = 1$) due to cancellation of the second order terms. Also, the errors for the 1 mm × 1 mm case are much less than those in Fig. 13(a) for a similar case. This is a result of the fact that the geometric center correctly represents the center of gravity of a rectangular winding.
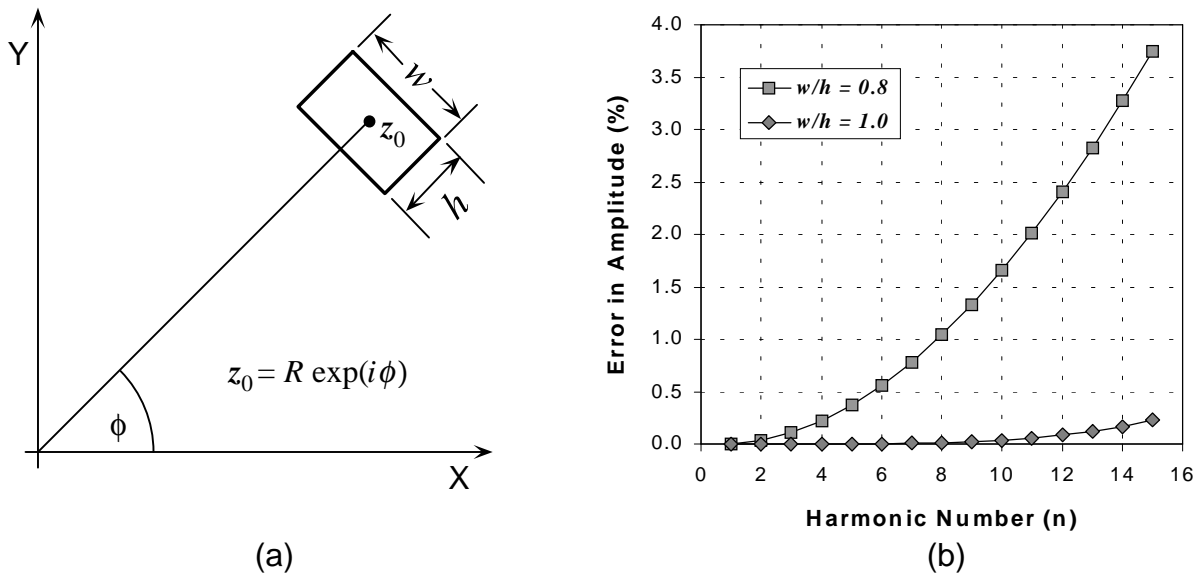

Fig. 14   (a) a winding with a rectangular cross section, and (b) errors in harmonic amplitudes for a 1 mm^2 winding size with different aspect ratios for $R = 10$ mm.

8.2 Random variation in the winding radius

For a well constructed coil, it is essential that all the geometric parameters of the coil be maintained uniform along the length of the coil. In practice, there may be random variations in these geometric parameters. We shall study in this, and the next few subsections, the effect of such random variations along the length.

Let us first consider the case of a random variation in the coil radius. We consider one segment of the coil loop in either a radial or a tangential coil. The radius is assumed to vary randomly along the length L of the coil, as shown in Fig. 15, with a mean value of R_c and a standard deviation of σ_R. The effective sensitivity factor of the coil for the n-th order harmonic is proportional to the average value of R^n over the coil length. If $\varepsilon(z)$ is the deviation in the radius, $R(z)$, at axial position, z, from the mean radius, R_c, then we may write:

$$R(z) = R_c + \varepsilon(z); \quad \frac{1}{L}\int_0^L R(z)\,dz = R_c; \quad \int_0^L \varepsilon(z)\,dz = 0; \quad \sigma_R^2 = \frac{1}{L}\int_0^L [R(z) - R_c]^2\,dz \quad (55)$$

Assuming small errors, and using Eq. (55), we can write the average value of R^n as

$$\frac{1}{L}\int_0^L [R(z)]^n\,dz = \frac{R_c^n}{L}\int_0^L \left[1 + \frac{n}{R_c}\varepsilon(z) + \frac{n(n-1)}{2R_c^2}\varepsilon^2(z) + \cdots\right]dz \approx R_c^n\left[1 + \frac{n(n-1)}{2}\left(\frac{\sigma_R}{R_c}\right)^2\right] \quad (56)$$

The sensitivity factor for the n-th harmonic is given by:

$$\boldsymbol{K}_n \approx \boldsymbol{K}_n^{ideal}\left[1 + \frac{n(n-1)}{2}\left(\frac{\sigma_R}{R_c}\right)^2\right] \quad (57)$$

In order to keep the error in the amplitude of the $n = 15$ term less than 1%, we should have $\sigma_R \leq 10^{-2} R_c$. A somewhat tighter tolerance may be required if such a coil is to be used to determine the transfer function of a magnet of higher multipolarity, such as a dodecapole corrector magnet. Practical coils of radius ~20 mm or more are generally built with $\sigma_R \leq 10^{-3} R_c$, for which the errors calculated from Eq. (57) are negligible.
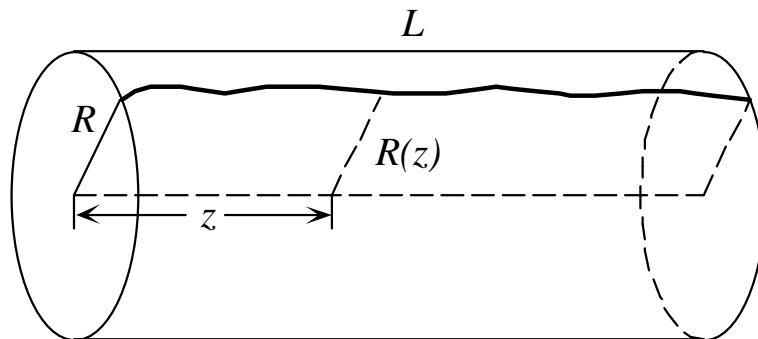

Fig. 15   Random variation in the winding radius along the length of the coil.

8.3 Random variation in the angular position (twist)

Let us consider the case of random variation in the angular position of the coil. The error will be derived for the specific case of a tangential coil in which the radii and opening angle are uniform along the length, but the angular position, δ, is assumed to vary randomly along the length L of the coil, as shown in Fig. 16, with a mean value of δ_c and a standard deviation of σ_δ. The case of a radial coil can be handled in an identical manner, and also yields an identical result. If $\varepsilon(z)$ is the deviation in the angular position at axial position, z, we may write

$$\delta(z) = \delta_c + \varepsilon(z); \quad \frac{1}{L}\int_0^L \delta(z)\,dz = \delta_c; \quad \int_0^L \varepsilon(z)\,dz = 0; \quad \sigma_\delta^2 = \frac{1}{L}\int_0^L [\delta(z) - \delta_c]^2\,dz \quad (58)$$

The flux seen by the tangential coil for the $2n$-pole field is [see Eq. (9)]:

$$\Phi_n(t) \propto \frac{1}{L}\int_0^L C(n)\sin(n\omega t + n\delta_c + n\varepsilon(z) - n\alpha_n)\,dz \quad (59)$$

Expanding $\sin[n\varepsilon(z)]$ and $\cos[n\varepsilon(z)]$ in power series and retaining only the terms up to the second order, it is easy to show that:

$$\Phi_n(t) \propto C(n)\sin(n\omega t + n\delta_c - n\alpha_n)\left[1 - \frac{n^2}{2}\sigma_\delta^2\right] \quad (60)$$

The sensitivity factor for the n-th harmonic is given by:

$$K_n \approx K_n^{ideal}\left[1 - \frac{n^2}{2}\sigma_\delta^2\right] \quad (61)$$

It should be noted from Eq. (61) that to a good approximation, the correction factor is a real quantity. This implies that the variation in angular position primarily leads to an error in the amplitude, and not the phase of a harmonic term, provided the mean angular position, δ_c, is accurately determined. The same result can be obtained starting from Eq. (5) for a radial coil.
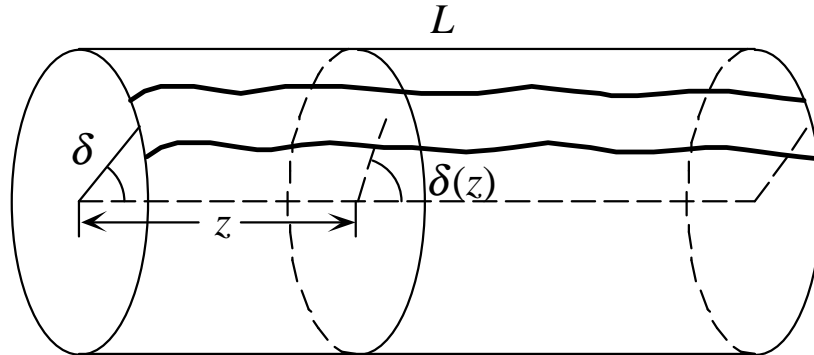

Fig. 16   Random variation in the angular position of a tangential coil.

8.4 Random variation in the opening angle of a tangential coil

While a radial coil is characterized by only the radii and the angular position, characterization of a tangential coil involves the opening angle also. For a long coil, this opening angle may vary along the length. Let us consider a tangential coil in which the radii and the angular position are uniform along the length. However, the opening angle, Δ, is assumed to vary randomly along the length L of the coil, as shown in Fig. 17, with a mean value of Δ_c and a standard deviation of σ_Δ. If $\varepsilon(z)$ is the deviation in the opening angle at axial position, z, we may write

$$\Delta(z) = \Delta_c + \varepsilon(z); \quad \frac{1}{L}\int_0^L \Delta(z)\,dz = \Delta_c; \quad \int_0^L \varepsilon(z)\,dz = 0; \quad \sigma_\Delta^2 = \frac{1}{L}\int_0^L [\Delta(z) - \Delta_c]^2\,dz \quad (62)$$

The flux seen by the coil for the $2n$-pole field is [see Eq. (9)]:

$$\Phi_n(\theta) \propto \frac{1}{L}\int_0^L \sin\left(\frac{n\Delta(z)}{2}\right)dz \quad (63)$$

Substituting for $\Delta(z)$ from Eq. (62), expanding $\sin[n\varepsilon(z)/2]$ and $\cos[n\varepsilon(z)/2]$ in power series and retaining only up to the second order terms, it is easy to show that:

$$\Phi_n(\theta) \propto \sin\left(\frac{n\Delta_c}{2}\right)\left[1 - \frac{n^2}{8}\sigma_\Delta^2\right] \quad (64)$$

The sensitivity factor for the n-th harmonic is given by:

$$K_n \approx K_n^{ideal}\left[1 - \frac{n^2}{8}\sigma_\Delta^2\right] \quad (65)$$

It is seen from Eqs. (61) and (65) that the measured amplitude of a given harmonic is more sensitive to random variations in the angular position than to random variations in the opening angle.
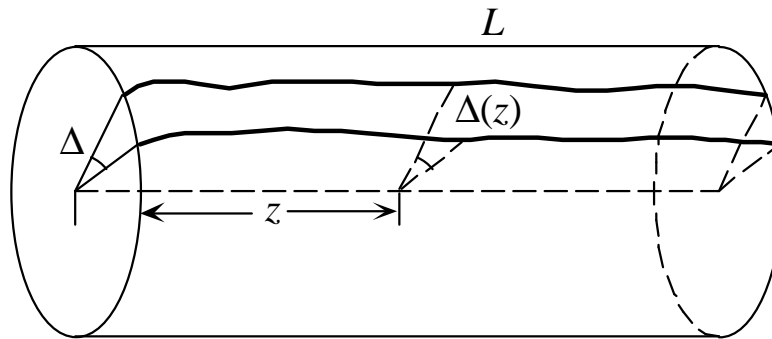

Fig. 17 Random variation in the opening angle of a tangential coil. The radii and the angular position are assumed to be constant along the length.

8.5   A tilt in the plane of a tangential coil

Ideally, the plane of a tangential coil should be perpendicular to the radial vector through the center of the coil. In practice, the two grooves used for winding the coil may not be at the same radius (e.g., in the method used at BNL), or the coil may be imperfectly mounted (e.g., in the method used at CERN), resulting in a slight tilt of the plane of the coil, as shown in Fig. 18. Even with a perfectly built coil, such an imperfection will be apparent if the rotation axis does not exactly coincide with the geometric center of the windings. Let us assume that the wires are located at radii of $R_c - \varepsilon$ and $R_c + \varepsilon$, as shown in Fig. 18. The general expression for the sensitivity factor of any rotating coil was derived in Sec. 5, and is given by Eq. (24). In the case of an imperfect tangential coil with unequal radii, we may write,

$$z_{1,0} = (R_c - \varepsilon)\exp(i\Delta/2); \quad z_{2,0} = (R_c + \varepsilon)\exp(-i\Delta/2) \tag{66}$$

$$z_{2,0}^n - z_{1,0}^n = (R_c + \varepsilon)^n \exp(-in\Delta/2) - (R_c - \varepsilon)^n \exp(in\Delta/2)$$
$$\approx 2R_c^n\left[-i\sin\left(\frac{n\Delta}{2}\right) + \left(\frac{n\varepsilon}{R_c}\right)\cos\left(\frac{n\Delta}{2}\right)\right] \tag{67}$$

The first term on the right hand side in Eq. (67) is related to the sensitivity of the perfect tangential coil [see Eq. (27)]. The second term implies that both amplitude and phase errors are introduced in the sensitivity factor. Also, for coils such as the dipole coil with $\Delta = \pi$, the flux for a perfect coil is zero for even harmonics. This is no longer the case with an imperfect coil. However, the allowed terms for a dipole coil ($\Delta = \pi$) are not affected since $\cos(n\pi/2) = 0$ for odd values of n. Assuming that $\sin(n\Delta/2)$ is not zero, as is the case for the harmonics of interest in a practical tangential coil ($\Delta \approx 15°$), we may write:

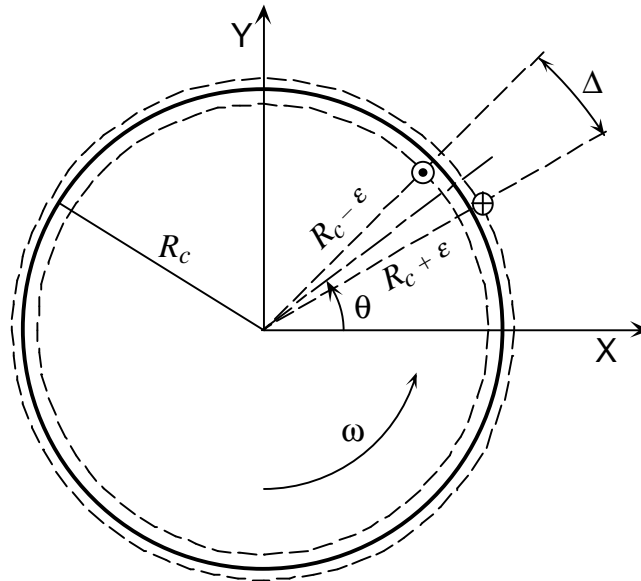$$\boldsymbol{K}_n \approx \boldsymbol{K}_n^{ideal} A_n \exp(in\lambda_n) \tag{68}$$

Fig. 18   A tilt in the plane of a tangential coil, resulting in (or resulting from) unequal radii for the two grooves of the winding.

where A_n is an amplitude correction factor and λ_n is a phase error given by:

$$A_n = \sqrt{1+\left(\frac{n\varepsilon}{R_c}\right)^2 \cot^2\left(\frac{n\Delta}{2}\right)} \approx 1 + \frac{n^2}{2}\left(\frac{\varepsilon}{R_c}\right)^2 \cot^2\left(\frac{n\Delta}{2}\right) \tag{69}$$

$$\lambda_n = \left(\frac{1}{n}\right)\tan^{-1}\left[\left(\frac{n\varepsilon}{R_c}\right)\cot\left(\frac{n\Delta}{2}\right)\right] \approx \left(\frac{\varepsilon}{R_c}\right)\cot\left(\frac{n\Delta}{2}\right) \tag{70}$$

The amplitude error is of the second order in (ε/R_c) and can generally be neglected. For typical values of $(\varepsilon/R_c) \sim 10^{-3}$, the phase error could be several milli-radians for the lowest order harmonics. The phase error reduces with the order of the harmonic as roughly $(1/n)$. This harmonic dependent phase error makes a calibration of the angular position difficult, because the apparent initial angular position of the coil measured in a dipole field will be different from that measured in a quadrupole field. In fact, such a discrepancy in the two calibrations can be used to estimate the tilt in the plane of the coil (see Sec. 10.1.2) as part of the coil calibration procedure. One can then use the sensitivity factor given by Eq. (68) to account for this tilt. Such a calibration and analysis procedure allows one to tolerate much larger construction errors than would be acceptable otherwise. An interesting observation from Eqs. (69) and (70) is that allowed harmonics in multipole coils (of the type discussed in Sec. 4) are insensitive to this type of error because $\cot(n\Delta/2)$ is zero.

8.6   A tilt in the plane of a radial coil

Similar to the case of a tangential coil discussed in the previous subsection, there can be a tilt in the plane of a radial coil from the ideal position. Such a tilt for a radial coil is shown in Fig. 19. The two ends of the coil are located at radii R_1 and R_2, and at two different angular positions, $\theta - \varepsilon$ and $\theta + \varepsilon$, instead of at a fixed angle θ. In this case, we may write,

$$z_{1,0} = R_1 \exp(-i\varepsilon); \quad z_{2,0} = R_2 \exp(i\varepsilon) \tag{71}$$

The sensitivity factor for such a coil is given by

$$\boldsymbol{K}_n = \frac{NLR_{ref}}{n}\left[\left\{\left(\frac{R_2}{R_{ref}}\right)^n - \left(\frac{R_1}{R_{ref}}\right)^n\right\}\cos(n\varepsilon) + i\sin(n\varepsilon)\left\{\left(\frac{R_2}{R_{ref}}\right)^n + \left(\frac{R_1}{R_{ref}}\right)^n\right\}\right] \tag{72}$$

The sensitivity factor is no longer a purely real quantity. Assuming a non-zero sensitivity factor for the ideal coil (i.e. $R_2^n - R_1^n \neq 0$) and small values of ε, we can write

$$\boldsymbol{K}_n \approx \boldsymbol{K}_n^{ideal} A_n \exp(in\lambda_n) \tag{73}$$

where A_n is an amplitude correction factor given by:

$$A_n = \sqrt{\cos^2(n\varepsilon) + \sin^2(n\varepsilon)\left(\frac{R_2^n + R_1^n}{R_2^n - R_1^n}\right)^2} \approx 1 + \frac{(n\varepsilon)^2}{2}\left[\left(\frac{R_2^n + R_1^n}{R_2^n - R_1^n}\right)^2 - 1\right] \tag{74}$$
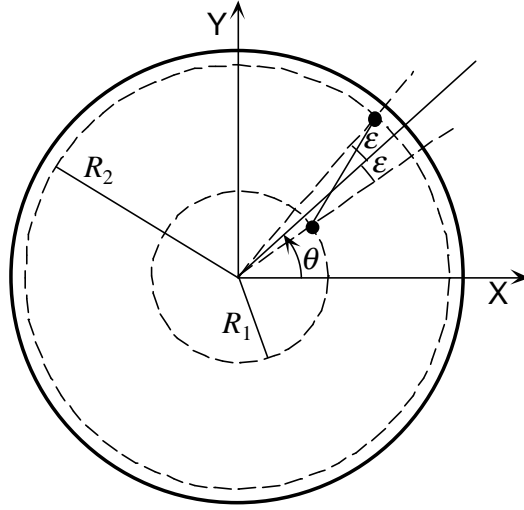
Fig. 19   A tilt in the plane of a radial coil.

and λ_n is the phase error for the $2n$-pole harmonic given by

$$\lambda_n = \left(\frac{1}{n}\right)\tan^{-1}\left[\tan(n\varepsilon)\frac{R_2^n + R_1^n}{R_2^n - R_1^n}\right] \approx \varepsilon.\left(\frac{R_2^n + R_1^n}{R_2^n - R_1^n}\right) \qquad (75)$$

The amplitude error is of the second order in ε, and can be neglected in practice. For $|R_1| \sim |R_2|$, the phase error may be several times ε for the lower order terms and has a limiting value of ε for sufficiently higher harmonics. As was mentioned in the previous subsection, a tilt in the plane of a radial coil will make the calibration of the initial angular position dependent on the multipolarity of the field used. Once again, this fact can be used to calibrate such a tilt and then correct the analysis for this effect. For the special case of a dipole coil with $R_1 = -R_2$, it can be seen that the errors are zero for all the allowed harmonics. This result is similar to that for a tilt in the plane of tangential coils.

8.7   An offset in the rotation axis

A coil assembly may be built perfectly, but the drive mechanism that rotates the coil may be misaligned with the geometric center of the coil. As was mentioned earlier, the effect of such an offset in the rotation axis is equivalent to a tilt in the plane of the coil, which has been discussed in the previous two subsections. If the radii and angular positions are calibrated with the rotating system already in place, then one need not consider the offset of the rotation axis as a separate imperfection. However, if one is using the design values of the coil parameters, then the effect of the offset in the rotation axis should be estimated.

Fig. 20(a) shows a general type of rotating coil with the initial positions of the wires given by $z_{1,0}$ and $z_{2,0}$ with respect to the geometric center as the origin. The rotation axis is assumed to be offset from the geometric center by a vector Δz_0 in the complex plane. We have

$$\boldsymbol{K}_n \propto \left[(z_{2,0} + \Delta z_0)^n - (z_{1,0} + \Delta z_0)^n\right]; \quad \boldsymbol{K}_n^{ideal} \propto \left[z_{2,0}^n - z_{1,0}^n\right] \qquad (76)$$

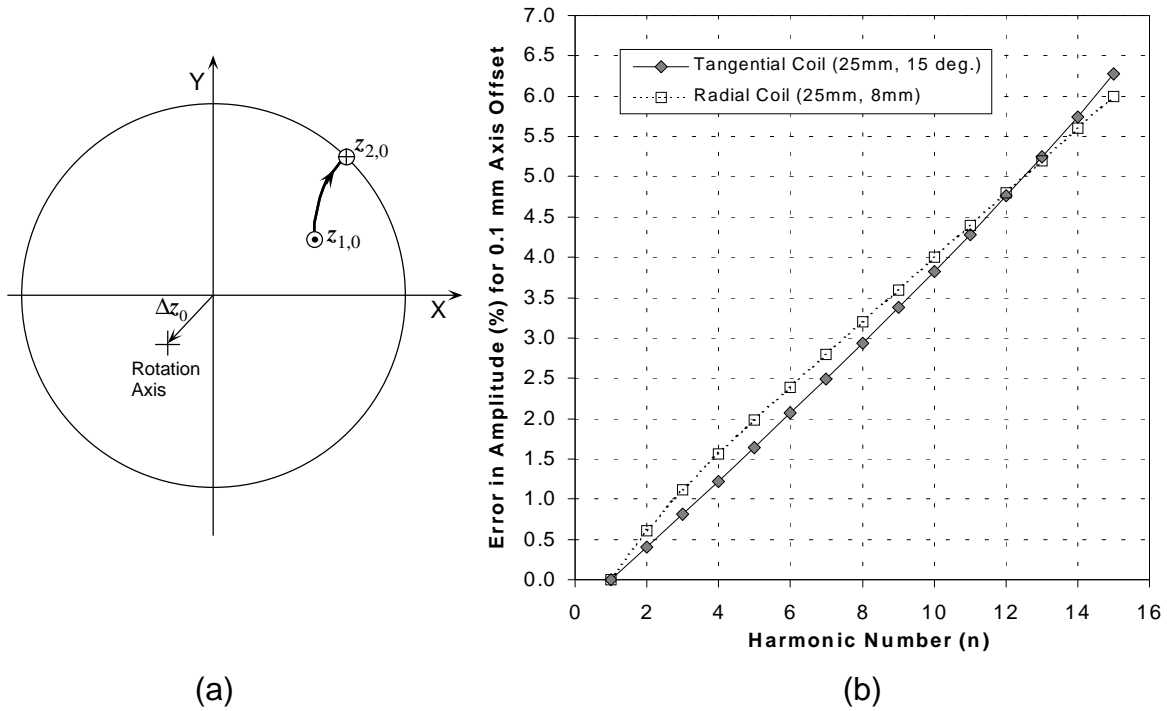(a)   (b)

Fig. 20   (a) An offset in the rotation axis, (b) percent errors in the amplitudes of various
harmonics with a 0.1 mm offset in the rotation axis. The tangential coil is assumed
to have a radius of 25 mm and an opening angle of 15 degrees, while the radial coil
is assumed to have radii $R_2 = 25$ mm and $R_1 = 8$ mm ($\sim R_1/3$).

If $\Delta \boldsymbol{K}_n = (\boldsymbol{K}_n - \boldsymbol{K}_n^{ideal})$ is the error in the sensitivity factor for the $2n$-pole term, then it can be
shown that

$$\left(\frac{\Delta \boldsymbol{K}_n}{\boldsymbol{K}_n}\right)_{\text{tangential}} = \sum_{k=1}^{n-1}\left[\frac{n!}{k!(n-k)!}\right]\left(\frac{\Delta z_0}{R_c}\right)^k \frac{\sin\left(\frac{(n-k)\Delta}{2}\right)}{\sin\left(\frac{n\Delta}{2}\right)} \tag{77}$$

$$\left(\frac{\Delta \boldsymbol{K}_n}{\boldsymbol{K}_n}\right)_{\text{radial}} = \sum_{k=1}^{n-1}\left[\frac{n!}{k!(n-k)!}\right](\Delta z_0)^k \frac{R_2^{n-k} - R_1^{n-k}}{R_2^n - R_1^n} \tag{78}$$

Usually, the offset is expected to be only a very small fraction of the coil radii. Consequently,
a first order approximation is adequate:

$$\left(\frac{\Delta \boldsymbol{K}_n}{\boldsymbol{K}_n}\right)_{\text{tangential}} \approx n\left(\frac{\Delta z_0}{R_c}\right)\frac{\sin\left[\frac{(n-1)\Delta}{2}\right]}{\sin\left[\frac{n\Delta}{2}\right]}; \quad \left(\frac{\Delta \boldsymbol{K}_n}{\boldsymbol{K}_n}\right)_{\text{radial}} \approx n(\Delta z_0)\left[\frac{R_2^{n-1} - R_1^{n-1}}{R_2^n - R_1^n}\right] \tag{79}$$

Eq. (79) may be used to estimate the tolerance on the alignment of the rotation axis with
the geometric axis for a desired degree of accuracy in the measurement of harmonics. These
results may also be used to estimate the effect of a "bow" or a bend in the measuring coil.
Different sections of such a coil will rotate about an axis which is offset from the geometric

center by different amounts. An approximate upper bound on the resulting effect can be obtained by equating Δz_0 to the total bend in the measuring coil, while an integration of Eq. (79) over the actual profile of the measuring coil should be used for a more accurate estimate. The estimated errors due to a 0.1 mm offset in the rotation axis are shown in Fig. 20(b) for a tangential and a radial coil with typical dimensions.

8.8   Systematic errors in the estimation of coil parameters

The coil parameters of primary interest are the radius (R), the angular position at the start of the data acquisition (δ), and in the case of a tangential coil, the opening angle (Δ). A systematic error in the knowledge of these parameters will result in systematic errors in the calculation of the field parameters, namely the amplitudes $C(n)$ and the phase angles α_n. Such errors would arise, for example, when the as-built coil has dimensions different from the design values, but the design values are used in the analysis. With a good calibration procedure, the effect of systematic errors can be practically eliminated. The only exception is in the case of analog bucking (see Sec. 7.4), where systematic errors can result in very poor bucking ratios unless amplifiers/resistors are used.

8.8.1 Systematic error in the radius

The sensitivity factor for the $2n$-pole field is proportional to R^n. Therefore, the error in the sensitivity factor due to a systematic error, ΔR, in the radius is given by

$$\frac{\Delta K_n}{K_n} = n\left(\frac{\Delta R}{R}\right) \tag{80}$$

For a ($\Delta R/R$) ~ 10^{-3}, the systematic error in the amplitude of the 20-pole term will be ~ 1%. Such an error is quite acceptable for the higher harmonics. The tolerance on the error in the knowledge of the radius arises primarily from considerations of the accuracy required in the measurement of the transfer function in the main dipole and quadrupole magnets in an accelerator and the desirability of consistency between different measuring systems.

8.8.2 Systematic error in the angular position

A systematic error, ε_δ, in the initial angular position, δ, leads to the same error in the determination of all the phase angles. This would give rise to skew terms in a purely normal magnet, and vice versa.

$$\alpha'_n = \alpha_n - \varepsilon_\delta; \quad C'(n)\exp(-in\alpha'_n) = C(n)\exp(-in\alpha_n)\left[\cos(n\varepsilon_\delta) + i\sin(n\varepsilon_\delta)\right] \tag{81}$$

where the primed quantities refer to the measured values and the unprimed quantities refer to the true values. The normal and skew multipoles in a magnet are generally expressed in a reference frame where the main field component has a zero phase angle. In this case, there will be no systematic error in the multipoles, since the phase angles relative to the main field still remain the same. However, when accurate determination of the field direction of the main component is required, such a systematic error is unacceptable. Efforts must be made to periodically check the calibration, and/or correct for the errors by making measurements from the lead and the non-lead ends of the magnet. A $2m$-pole magnet with a true phase angle of α_m when viewed from the lead end, has a phase angle of $[1+(-1)^m](\pi/2m) - \alpha_m$ when viewed from

the non-lead end. The measured phase angles from the lead and the non-lead ends in the presence of a systematic error in the angular position are:

$$\alpha_{\text{lead}} = \alpha_m - \varepsilon_\delta; \quad \alpha_{\text{non-lead}} = \left[1 + (-1)^m\right]\left(\frac{\pi}{2m}\right) - \alpha_m - \varepsilon_\delta \qquad (82)$$

From these two measured values, it is easy to see that the true phase angle, α_m, is given by

$$\alpha_m = \left(\tfrac{1}{2}\right)\left[\alpha_{\text{lead}} - \alpha_{\text{non-lead}} + \{1 + (-1)^m\}\left(\tfrac{\pi}{2m}\right)\right] \qquad (83)$$

and the systematic error in the angle is given by

$$\varepsilon_\delta = \left(\tfrac{1}{2}\right)\left[\{1 + (-1)^m\}\left(\tfrac{\pi}{2m}\right) - \alpha_{\text{lead}} - \alpha_{\text{non-lead}}\right] \qquad (84)$$

Having determined the systematic error in the angle from Eq. (84), the correction can be incorporated by adjusting the parameter δ accordingly in all the future analysis. It is generally a good idea to carry out periodic checks of this calibration whenever a reliable measurement of the field angle is required.

8.8.3 Systematic error in the opening angle of a tangential coil

The sensitivity factor, K_n, of a tangential coil [see Eq. (27)] depends on the opening angle, Δ, through the $\sin(n\Delta/2)$ factor. For a systematic error ε_Δ in the opening angle,

$$\frac{\Delta K_n}{K_n} = \left(\frac{n}{2}\right)\cot\left(\frac{n\Delta}{2}\right)\varepsilon_\Delta \qquad (85)$$

This error is generally insignificant for higher order harmonics. In a typical tangential coil system, the dipole and the quadrupole terms are obtained from the dipole ($\Delta = 180$ degrees) and the quadrupole ($\Delta = 90$ degrees) windings respectively. It is seen from Eq. (85) that such *multipole coils* ($\Delta = \pi/n$) are insensitive to small errors in the opening angle.

8.9 Effect of a finite signal averaging time

In the acquisition of voltage data from the RHIC tangential coils, the signals are averaged over one power line cycle to get rid of any AC noise on the signals. At a typical angular speed of one revolution every 3.5 seconds and a power line frequency of 60 Hz, the coil rotates about 1.7 degrees during this time. This motion during data integration can cause errors. Even though this does not strictly fall under construction errors, a finite integration time manifests itself in some sense as a calibration error, as we shall see. Accordingly, this topic is discussed in this section as part of the general discussion on coil errors.

We shall consider the case of a tangential coil here, although a similar result can be derived for radial coils also. If Δt is the averaging time, the n-th harmonic component in the measured voltage signal is [see Eq. (10)]:

$$V_n(t) \propto \frac{1}{\Delta t}\int_t^{t+\Delta t}\cos(n\omega t + n\delta - n\alpha_n)\,dt = \frac{\sin(n\omega\Delta t/2)}{n\omega\Delta t/2}\cos\left[n\omega t + n\left(\delta + \frac{\omega\Delta t}{2}\right) - n\alpha_n\right] \quad (86)$$

It is seen that both the amplitude and the phase of the 2*n*-pole term are affected. While the amplitude correction is harmonic dependent, the phase correction is independent of the harmonic. The constant phase error can be absorbed into the calibration of the initial angular position, δ. From Eq. (86), we can write,

$$\text{Amplitude Correction Factor} = \frac{\sin(n\omega\Delta t/2)}{n\omega\Delta t/2} \approx 1 - 1.64n^2\left(\frac{\Delta t}{T}\right)^2 \tag{87}$$

$$\text{Effective Angle Calibration} = \delta' = \delta + (\omega\Delta t/2) = \delta + \pi\left(\frac{\Delta t}{T}\right) \tag{88}$$

where T is the period of rotation. For $\Delta t = 1/60$ sec. and $T = 3.5$ sec, $(\Delta t/T) \sim 4.8\times10^{-3}$, the amplitude error is 0.004% for the dipole term and is 0.84% for the 30-pole term. This effect is negligible. However, the angle calibration is affected by roughly 0.86 degrees (15 mrad). Fortunately, the error is harmonic independent, and can be absorbed in the calibration of the coil, *as long as the angular velocity is kept the same*. Considerable error will result, for example, if the coil were to rotate in the opposite direction ($\omega \to -\omega$).

In practice, the coil rotation period may not be exactly the same during calibration and measurements. It is necessary, therefore, to specify the rotation speed of the measuring coil along with the angular parameters. Corrections must be applied to the calibration values based on the actual rotation speed during the measurements according to the above equations if accuracy in the range of 0.1 mrad is desired in the field angle.

9.   DEVIATION OF THE ROTATION AXIS FROM THE MAGNETIC AXIS

In the previous section, we considered the effects of various random and systematic errors in the construction of a rotating coil. The harmonic expansion parameters in Eq. (1)-(3) are dependent on the choice of the coordinate axis [1]. In the analysis of harmonic coil data, it is assumed that the origin is at the rotation axis. In the measurement of an accelerator magnet, one is generally interested in the harmonics at the magnetic center. Unless special effort is made, the rotation axis of the coil may not coincide with the magnetic axis. In this section, we shall study the effect of a misalignment of the rotation axis with the magnetic axis. Three different forms of misalignment will be considered – a simple offset, a sag of the measuring coil due to its own weight, and a tilt of the rotation axis with respect to the magnet axis.

9.1   Rotation axis offset from the magnetic axis

Let us first assume that the rotation axis is parallel to the magnetic axis, but is not coincident with it. This is the most common form of misalignment in practice. This is also the most important form of misalignment because the measured harmonic coefficients are affected by feed down. Figure 21 shows the measuring coil reference frame, *X-Y*, with the origin at the rotation axis passing through *O*, and the desired reference frame, *X'-Y'*, with the origin at the magnetic axis passing through *O'*, located at (x_0, y_0) in the *X-Y* frame.

If $C(n)$ and α_n are the measured parameters in the measuring coil frame, then the parameters $C'(n)$ and α'_n in the magnet's frame are given by [1]:
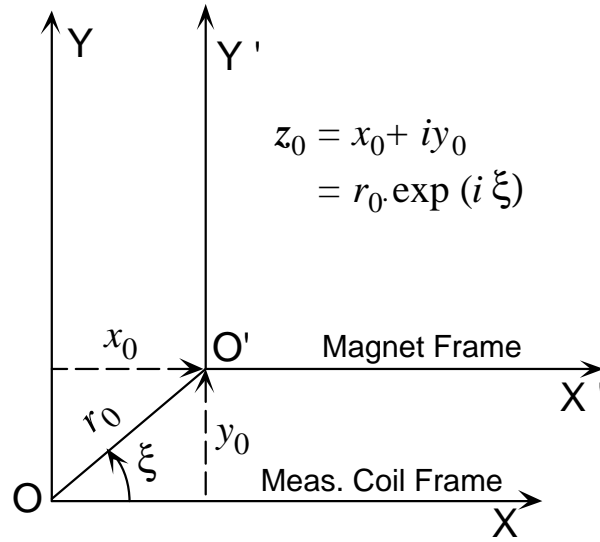
Fig. 21   Displacement of the measuring coil axis from the magnetic axis.

$$C'(n)\exp(-in\alpha'_n) = \sum_{k=n}^{\infty} C(k)\exp(-ik\alpha_k)\frac{(k-1)!}{(n-1)!(k-n)!}\left(\frac{z_0}{R_{ref}}\right)^{k-n} \tag{89}$$

If the offset $z_0 = (x_0 + iy_0)$ is somehow known, one can account for the misalignment by calculating the field parameters in the magnet's frame using Eq. (89).

9.1.1 Magnets other than dipole magnets

For a $2m$-pole magnet other than a dipole, it is quite natural to define the magnetic center as the location where the $2(m-1)$- pole feed down term is zero. Thus, the offset itself can be calculated from the measured harmonics using the following equation derived from Eq. (89):

$$C'(m-1)e^{-i(m-1)\alpha'_{m-1}} = C(m-1)e^{-i(m-1)\alpha_{m-1}} + (m-1)C(m)e^{-im\alpha_m}\left(\frac{z_0}{R_{ref}}\right)$$

$$+\frac{m(m-1)}{2}C(m+1)e^{-i(m+1)\alpha_{m+1}}\left(\frac{z_0}{R_{ref}}\right)^2 + \frac{m(m^2-1)}{6}C(m+2)e^{-i(m+2)\alpha_{m+2}}\left(\frac{z_0}{R_{ref}}\right)^3 +\cdots= 0 \tag{90}$$

For most $2m$-pole magnets, amplitudes other than $C(m)$ are small. For small offsets, we may neglect higher order terms in (z_0/R_{ref}) and use a simplified equation:

$$\left(\frac{z_0}{R_{ref}}\right) \approx -\frac{1}{(m-1)}\frac{C(m-1)\exp\{-i(m-1)\alpha_{m-1}\}}{C(m)\exp(-im\alpha_m)}; m \neq 1; |z_0| << R_{ref} \tag{91}$$

Once the offset is calculated from Eq. (90) or (91), the measured data can be transformed using Eq. (89) to obtain the field parameters in the desired reference frame. This procedure of transforming the measured data to the magnet's reference frame is commonly referred to as the *centering of data*.

9.1.2 Dipole magnets

For dipole magnets, the field is practically uniform in the entire magnet aperture and no "natural" definition of a magnetic center can be used. Various strategies are used to define the center of a dipole magnet. For example, one could argue that the very high order *unallowed* terms are not sensitive to small construction errors, and hence must be zero. In practice, this certainly appears to be the case for any carefully built accelerator dipole magnet. If so, one could pick m in Eq. (90) to be a sufficiently high order *allowed* term and calculate the center by requiring the amplitude of the next lower *unallowed* term, $C'(m–1)$, to be zero. Of course, this works well only if $C(m)$ itself has sufficient strength. Because of the large values of m, the measured coefficients are of comparable strengths for both the allowed and the unallowed harmonics, even with relatively small offsets. As a result, it is often necessary to include terms of higher orders in (z_0/R_{ref}) to calculate the offset. In many cases, ambiguous, yet physically meaningful, results may be obtained because of the non-linear nature of the equations. To resolve this, it is best to find an offset that will simultaneously minimize several unallowed harmonics, rather than just one.

Other strategies for dipoles have exploited a current dependence of the sextupole term. Such a current dependence may arise from non-uniform saturation of the iron yoke at high fields, or from the magnetization of the superconductor at relatively low fields in a superconducting magnet. The quadrupole term at the magnetic center is not expected to show any current dependence. However, if the measuring coil axis does not coincide with the magnetic axis, a current dependence will be seen due to feed down from the sextupole term. Thus, the offset of the measuring coil can be obtained by requiring that the current dependence of the quadrupole multipole be minimized. In practice, one may find that the calculated center depends on the range of the excitation curve used in the minimization. In some cases, the current dependence in the quadrupole term may not be entirely due to feed down. For example, the critical currents of the superconducting cables used for the upper and the lower coils may be slightly different, leading to a current dependence in the quadrupole multipole at low fields. Such effects may limit the accuracy achievable with this technique. Furthermore, this technique can not be used for warm measurements at low fields.

9.1.3 The quadrupole configured dipole ("ugly quad") method for dipole magnets

The methods discussed so far for dipole magnets have inherent limitations and are not universally applicable. A different approach, known as the quadrupole configured dipole (QCD) or an "ugly quad" method, was proposed for centering in the SSC dipoles [11]. Subsequently, the method was adopted for all the RHIC dipoles and has been used with much success for measurements of magnets in both warm and superconducting state.

The quadrupole configured dipole method relies on powering the two coil halves of a dipole magnet with equal and opposite currents, as shown in Fig. 22, to produce a strong skew quadrupole field, instead of a dipole field. This requires a center tap connection on the magnet. The allowed harmonics are now the skew quadrupole, skew octupole, skew dodecapole, and so on. Several of these allowed harmonics are quite strong, and feed down from any one of them could be used to calculate the center. Since the quadrupole field produced in this way has large octupole and higher harmonics, the method is sometimes referred to as the "ugly quad" method.
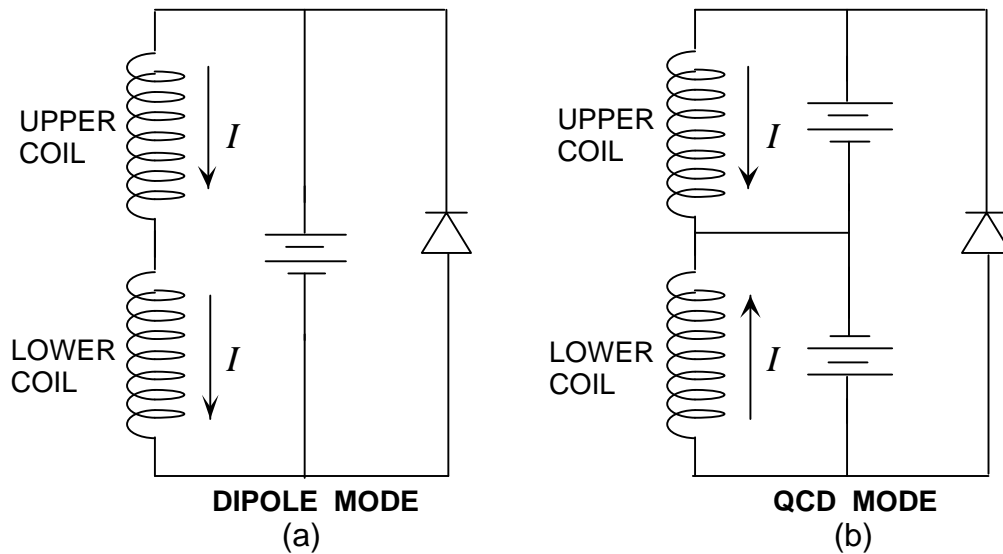
Fig. 22   A dipole magnet powered in the (a) dipole mode, and (b) the QCD mode. The diode shown is for quench protection. The diode and the current polarities shown are for warm measurements.

Since two separate power supplies are required in this mode, it is important to balance the current in the two halves with great accuracy, otherwise a spurious dipole field will also be generated that would affect centering calculations. The sensitivity to such a current mismatch is reduced by several orders of magnitude if one uses feed down from the skew octupole term, or any other higher order term, rather than the dominant skew quadrupole term. Matching the currents in the two halves within 0.1% will give a centering error of less than a few micro-meters in this case. The offsets calculated from the QCD method have very little noise (typically only a few micro-meters) and are in very good agreement with the centers calculated by making high order unallowed terms zero.

9.2   Sag of the measuring coil due to its own weight

In order to measure precisely the integral field in long magnets, one has to build long rotating coils. For such long measuring coils, the weight of the cylindrical tube containing the coil may be enough to cause a sagitta in the coil. In this case, each subsection of the coil rotates about its local geometric center. However, the location of this center varies along the length of the magnet, as shown by the dashed line in Fig. 23. This is different from a "bow" or bend in the coil, in which all sections of the coil rotate about the same *straight line* axis, but the axis is offset from the geometric center by different amounts along the length of the coil. The case of a bend in the coil was discussed briefly in Sec. 8.7. In the case of a sag of the coil, various subsections of the coil see harmonics that are in a frame which is slightly displaced from the adjacent subsections. If $r_0(Z)$ is the vertically downward offset at axial position Z, the measured coefficients are given by:

$$C'(n)\exp(-in\alpha'_n) = \sum_{k=n}^{\infty} C(k)\exp(-ik\alpha_k)\frac{(k-1)!\exp\left\{-i(k-n)\frac{\pi}{2}\right\}}{(n-1)!(k-n)!}\left(\frac{1}{L}\right)\int_{-L/2}^{L/2}\left(\frac{r_0(Z)}{R_{ref}}\right)^{k-n} dZ \quad (92)$$
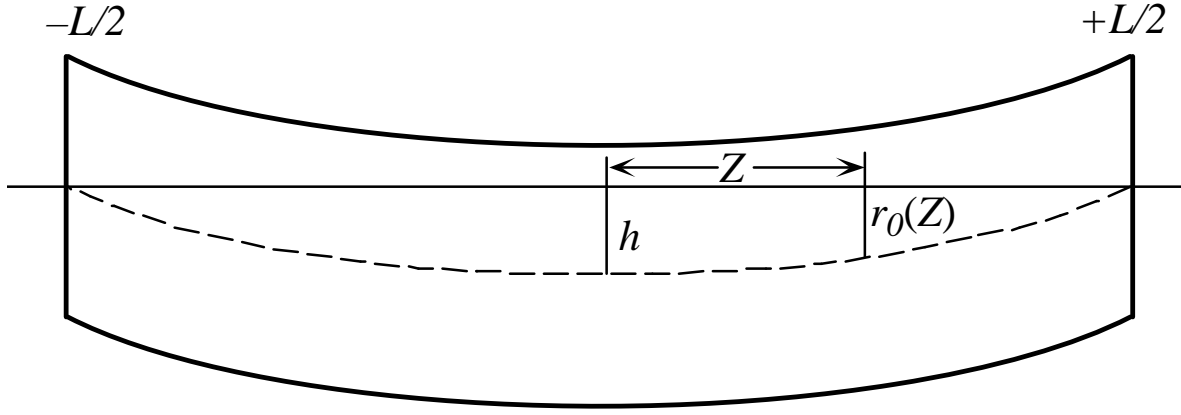
Fig. 23   Sag of a measuring coil due to its own weight.

where $C(k)$ and α_k are the true field parameters. Equation (90) has been used in writing Eq. (92) where the offset z_0 is vertically downward, and is a function of the axial position Z:

$$z_0(Z) = r_0(Z)\exp(-i\pi/2) \tag{93}$$

If the profile of the coil is known, the integral in Eq. (92) can be evaluated to estimate the effect of the sag on various harmonics. Assuming a parabolic approximation to the profile given by

$$r_0(Z) = h\left[1 - \frac{Z^2}{(L/2)^2}\right]; \quad -\frac{L}{2} \le Z \le \frac{L}{2} \tag{94}$$

where h is the amount of sag at the center of the coil ($Z = 0$), it can be shown [12] that:

$$C'(n)\exp(-in\alpha'_n) = \sum_{k=n}^{\infty} C(k)\exp(-ik\alpha_k) \frac{(k-1)!\exp\left\{-i(k-n)\frac{\pi}{2}\right\}}{(n-1)!(k-n)!} \frac{[2(k-n)]!!}{[2(k-n)+1]!!}\left(\frac{h}{R_{ref}}\right)^{k-n} \tag{95}$$

where $(2k)!! = 2.4.6.8. \ldots 2k, \; (2k+1)!! = 1.3.5. \ldots (2k+1)$ and $0!! = 1$.

The error in certain harmonics may be significant, even with small amounts of sag. However, for small values of h ($<<R_{ref}$), the effect of sag from Eq. (95) is nearly the same as a uniform displacement of the coil by an amount ($2h/3$), which is the average displacement of the sagging coil. If the measured data are corrected for any offset of the measuring coil axis, most of the errors due to sag are also subtracted out [3], except for terms of second and higher orders in (h/R_{ref}) which can be neglected for practical values of h. Thus, within reasonable limits, the sag of a measuring coil is not a problem for the measurement of harmonics, provided the data are centered using a reliable centering technique based on the measured harmonics, as described in Sec. 9.1. However, if the harmonic coil is being used specifically to measure the magnetic axis, for example in a quadrupole, even a relatively small sag in the coil may be unacceptable, because one can not distinguish between a *true offset* of the magnetic axis and an *apparent offset* due to the sag.

9.3   Tilt of the measuring coil axis relative to the magnet axis

If sufficient care is not taken in aligning the coil, the measuring coil axis can be tilted with respect to the magnetic axis. Generally, the clearance between the inner diameter of the magnet bore and the outer diameter of the coil assembly is kept sufficiently small, so that such a tilt can not be very large. In most cases, this tilt is not of much concern. However, in some situations, even a small tilt can have a significant impact on the measurement of certain harmonics. As a result, it is important to study this type of misalignment of the coil axis.

We shall consider a simple case in which the magnet has uniform field quality along the length, L, covered by the measuring coil. This would apply, for example, to measurements with a relatively short coil in the straight section of a magnet. We also assume a pure tilt, with the average offset of the measuring coil to be zero, as shown in Fig. 24. The displacements of the coil-axis at the two ends are assumed to be given by (r_0, ξ) and $(r_0, \xi+\pi)$ in polar coordinates. The measured harmonics can be calculated by integrating along the length using a procedure similar to that used for a sag of the coil in Sec. 9.2. If the field quality is uniform along the length, the odd orders of feed down from one half of the magnet will be cancelled by the corresponding feed down from the other half of the magnet. The even orders of feed down from the two halves will add to each other. The measured coefficients in this case are given by [3]:

$$C'(n)\exp(-in\alpha'_n) = \sum_{\substack{k=n \\ (k-n)=\text{even}}}^{\infty} \frac{C(k)\exp(-ik\alpha_k)}{(k-n+1)} \frac{(k-1)!}{(n-1)!(k-n)!} \left(\frac{r_0 \exp(i\xi)}{R_{ref}} \right)^{k-n} \quad (96)$$

It should be noted that the summation in Eq. (96) includes only those values of k for which $(k–n)$ is even. The lowest order correction term is of the second order in (r_0/R_{ref}), and can generally be neglected for dipole and quadrupole magnets, since there can not be any second order feed down from the main field component. The only errors will be due to second and higher order feed down from the higher harmonics, which are expected to be small themselves. However, for sextupoles and magnets of higher multipolarity, there can be a second order feed down from the main harmonic, leading to large errors even with a relatively small tilt. For example, the dipole field component will be incorrectly measured in a sextupole magnet, the quadrupole component in an octupole magnet, and so on.
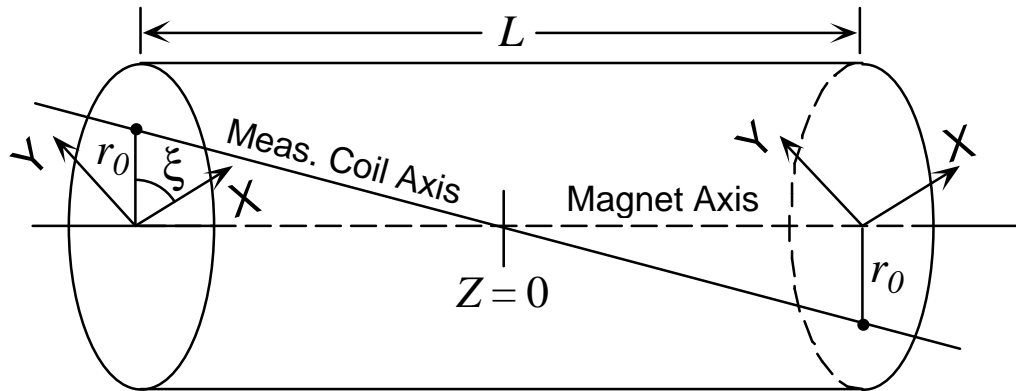

Fig. 24   Tilt of the measuring coil axis with respect to the magnet axis. The cylinder represents the section of the magnet covered by the length of the measuring coil
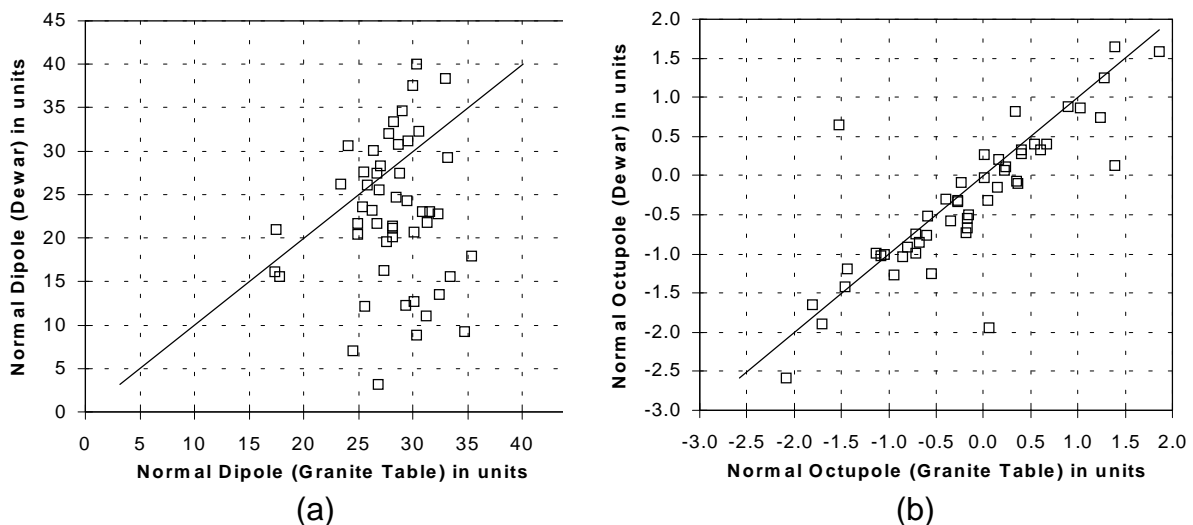
Fig. 25   Correlation between the harmonics measured in RHIC sextupoles in a well aligned fixture on a granite table and in a vertical dewar with a possible tilt in the coil — (a) the normal dipole term, which could be affected by the tilt, and (b) the normal octupole term, which is not affected by the tilt. The straight lines represent the case of a perfect agreement between the two measurements.

As a demonstration of the effect of tilt, Fig. 25 shows the correlation between harmonics measured in RHIC sextupoles with a well aligned coil on a granite table and with a possibly tilted coil in a vertical dewar. As explained above, the dipole term is expected to be affected by a tilt in the measuring coil axis. The correlation is indeed poor for the dipole term, as can be seen from Fig. 25(a). The difference between the two measurements is not a systematic one resulting from calibration errors, but is random depending upon the amount of tilt in the coil, and could be up to ±25 units. On the other hand, for the octupole term, which is not expected to be affected by such a tilt, the correlation between the two measurements is quite good, as shown in Fig. 25(b).

The above analysis assumed that the field quality of the magnet is uniform over the length of the measuring coil. Often, magnets may have rather large harmonics in the lead end region which are absent in the non-lead end region. In this case, if one is making an integral measurement with a long coil, even the first order terms from the two halves will not cancel each other, causing large errors. Examples of such errors are in the measurement of integral decapole terms in a quadrupole magnet having large dodecapole terms in the lead end region.

10.   CALIBRATION OF HARMONIC COILS

In the previous two sections, we studied the effects of various imperfections in the coil construction and placement. Analysis of such errors can be helpful in determining various tolerances. On the other hand, once a coil is constructed, it is important to characterize the geometric parameters of the various windings as precisely as possible. Most coil systems in use have special windings sensitive to the dipole and the quadrupole terms. The radii and angular positions of such windings can be determined if reference dipole and quadrupole magnets with known field strengths and directions are available. Having such magnets with apertures and lengths suitable for the coil being calibrated greatly simplifies the process of

calibration. In an accelerator, magnets of various lengths and apertures are used. Correspondingly, one needs to use a variety of measuring coils to measure these magnets. It may not always be practical to provide reference dipole and quadrupole magnets for all coil types. In such a situation, one has to obtain as much information about the coil geometry as possible, without requiring an explicit knowledge of the field strength or direction. The number of calibration parameters can be greatly reduced simply by comparing the outputs of various windings in a given field type. One must devise a scheme appropriate to the specific coil design at hand. The basic concept will be illustrated here with the example of the five-winding tangential coil design used at RHIC.

10.1 Calibration of a five-winding tangential coil

The cross-section of a five winding tangential coil design used at RHIC is shown in Fig. 9. There are two dipole buck windings (D1 and D2), two quadrupole buck windings (Q1 and Q2) and a tangential winding (T1) with an opening angle of 15 degrees. The radii of these windings are assumed to be given by R_1 through R_5. Similarly, the angular positions of the windings are assumed to be given by δ_1 through δ_5. In addition, one needs to know the exact opening angle, Δ, of the tangential winding. The nominal values of these eleven parameters are known from the design. However, the precise values of these parameters in the as-built coil may differ slightly from the design and must be obtained by a calibration procedure. In addition to these eleven parameters, it has been found necessary to account for a small tilt in the plane of the tangential coil, characterized by a parameter ε, which can give rise to a harmonic dependent correction in the angular position (see Sec. 8.5). Thus, there are a total of 12 parameters to be determined in this case. It will be shown here that one can determine all the angles relative to each other, all the radii relative to each other, the absolute value of the opening angle, as well as the tilt in the plane of the tangential coil — all by using dipole, quadrupole and sextupole fields whose strengths and field directions are not necessarily known. The absolute values of all the parameters can be obtained if just one of the field strengths and one of the field directions are known.

10.1.1   Calibration of the radii

Let the n-th harmonic amplitude in the voltage signal from the j-th winding be denoted by $V_j(n)$. In a dipole field, assuming a measuring coil longer than the magnet, the dipole amplitudes in the signals from D1, D2 and T1 windings are given by [see Eq. (10)]:

$$V_1(1) \propto N_1 R_1; \quad V_2(1) \propto N_2 R_2; \quad V_3(1) \propto N_3 R_3 \sin(\Delta/2) \tag{97}$$

where N_1, N_2 and N_3 are the number of turns in the three windings, and are assumed to be known. For measuring coils shorter than the magnet, one has to include the lengths of the windings also in the above equations. In general, the windings have lengths much larger than their radii. Thus, small errors in the lengths are not as critical as similar errors in the radii. Except for ultra short coils, one can assume the lengths to be given by the design value. Similarly, the opening angles of the two dipole buck windings can be safely assumed to be 180 degrees, since the quantity $\sin(n\Delta/2)$ is not very sensitive to small errors in Δ in this case. The quadrupole windings are not sensitive to the dipole field, and are expected to give practically zero signal in a dipole field. From Eq. (97), we have,

$$\left(\frac{R_2}{R_1}\right) = \left(\frac{V_2(1)}{V_1(1)}\right)\left(\frac{N_1}{N_2}\right); \quad \left(\frac{R_3}{R_1}\right)\sin\left(\frac{\Delta}{2}\right) = \left(\frac{V_3(1)}{V_1(1)}\right)\left(\frac{N_1}{N_3}\right) \tag{98}$$

Similarly, in a quadrupole field, the amplitudes of the quadrupole terms in the voltage signals from the Q1, Q2 and T1 windings are given by [see Eqs. (18) and (10)]:

$$V_4(2) \propto 2N_4 R_4^2; \quad V_5(2) \propto 2N_5 R_5^2; \quad V_3(2) \propto N_3 R_3^2 \sin(\Delta) \tag{99}$$

which leads to the ratios of radii,

$$\left(\frac{R_5}{R_4}\right) = \left[\left(\frac{V_5(2)}{V_4(2)}\right)\left(\frac{N_4}{N_5}\right)\right]^{1/2}; \quad \left(\frac{R_3}{R_4}\right)^2 \sin(\Delta) = \left(\frac{V_3(2)}{V_4(2)}\right)\left(\frac{2N_4}{N_3}\right) \tag{100}$$

The constants of proportionality in Eqs. (97) and (99) involve the field strengths and the angular velocity. The dependence on the angular velocity can be removed, in principle, by looking at the integral of the voltage signal. If the field strengths in the dipole and the quadrupole magnets are also known, one can obtain the absolute values of R_1, R_2, and R_4, R_5. From these values, the absolute values of R_3 and Δ can also be determined using the above equations. If the absolute strengths are not known, one can only calculate the ratios of radii. Even then, we have only four equations in five unknowns (four ratios of the radii and the opening angle) and need more information. If we use a sextupole field, then the D1, D2 and T1 windings are sensitive to this field. The amplitudes of the sextupole term in the signals are given by [see Eqs. (18) and (10)]:

$$V_1(3) \propto N_1 R_1^3; \quad V_2(3) \propto N_2 R_2^3; \quad V_3(3) \propto N_3 R_3^3 \sin(3\Delta/2) \tag{101}$$

which lead to the ratios

$$\left(\frac{R_2}{R_1}\right) = \left[\left(\frac{V_2(3)}{V_1(3)}\right)\left(\frac{N_1}{N_2}\right)\right]^{1/3}; \quad \left(\frac{R_3}{R_1}\right)^3 \sin(3\Delta/2) = \left(\frac{V_3(3)}{V_1(3)}\right)\left(\frac{N_1}{N_3}\right) \tag{102}$$

Eqs. (98), (100) and (102) provide enough information to calculate the five unknowns, namely, (R_2/R_1), (R_3/R_1), (R_4/R_1), (R_5/R_1) and Δ. We get one redundant equation, which could be used for consistency check on (R_2/R_1), or could be used for estimating the length errors in the case of a short coil. To know the absolute values of the radii, we need to independently determine just one radius. This could be obtained easily if a reference field is available. Otherwise, the radius of one of the windings has to be estimated from mechanical measurements. It is generally a good idea to choose the winding with the minimum number of layers of wire for such an estimation. If another well calibrated coil is available, the radii can also be calibrated against this coil.

10.1.2 Calibration of the angular positions

If reference dipole and quadrupole magnets are available with precisely known phase angles, the angular positions δ_1, δ_2, δ_4, and δ_5 can be easily determined from the phases of the dipole and the quadrupole components of the measured signals. Due to a possible tilt in

the plane of the tangential coil, the apparent angular position of the tangential winding, $\delta_3(1)$, determined in a dipole magnet will not be the same as the apparent angular position, $\delta_3(2)$, determined in a quadrupole magnet. These values, however, can be used to obtain the true angular position, δ_3^0, and the tilt parameter, (ε/R_3), using the relations (see Sec. 8.5):

$$\delta_3(n) = \delta_3^0 + \lambda_n; \qquad \lambda_n = \left(\frac{1}{n}\right) \tan^{-1}\left[\left(\frac{n\varepsilon}{R_c}\right)\cot\left(\frac{n\Delta}{2}\right)\right] \qquad (103)$$

If the absolute phase angles of both the dipole and the quadrupole fields are not known, we can not use Eq. (103) for calibration. In this case, we again make use of a sextupole field. In a dipole field, we can determine the quantities $\delta_2 - \delta_1$ and $\delta_3(1) - \delta_1$ from the observed phases of the dipole components of the voltage signals. Similarly, in a quadrupole field, we can determine the quantities $\delta_5 - \delta_4$ and $\delta_3(2) - \delta_4$. Finally, $\delta_2 - \delta_1$ and $\delta_3(3) - \delta_1$ are determined in a sextupole field.

Combining the data from the dipole and the sextupole fields, we get the quantity $\delta_3(3) - \delta_3(1)$, which depends on (ε/R_3) and the opening angle, Δ. Since Δ is obtained along with the calibration of the radii, the parameter (ε/R_3) is determined. Knowing (ε/R_3), one can calculate $\delta_3(2) - \delta_1$, which can be combined with the data in a quadrupole field to get δ_4 and δ_5 also relative to δ_1. All angles are thus known relative to one of the windings. For coils equipped with a gravity sensor, the absolute angles can be obtained by making measurements from the lead and the non-lead ends of a magnet (see Sec. 8.8.2). For other systems, such as for measurements in a vertical dewar, absolute values of angles are often unnecessary. The design value of δ_1 can be used in this case and all other angles can be determined from the procedure described here. All the parameters of interest for carrying out harmonic analysis using such a tangential coil are thus determined. As shown in this section, all the parameters relative to one of the windings can be obtained without any knowledge of the field strengths or directions of the magnets used for the calibration.

ACKNOWLEDGEMENTS

***

REFERENCES

[1] A. K. Jain, *Basic Theory of Magnets,* these proceedings.

[2] A. Devred and M. Traveria, *Magnetic Field and Flux of Particle Accelerator Magnets in Complex Formalism*, Report CRYOMAG/94/08, December 20, 1994, Centre d'Etudes de Saclay, 91191 Gif-sur-Yvette Cédex, France.

[3] A.K. Jain, *Effect of Measuring Coil Imperfections on the Measured Field Parameters*, Tech. Note AD/SSC/Tech. No. 99 (SSCL-N-784), January 2, 1992, Brookhaven National Laboratory, Upton, New York 11973.

[4] W.G. Davis, *The Theory of the Measurements of Magnetic Multipole Fields with Rotating Coil Magnetometers*, Nucl. Instrum. Meth. in Physics Research, **A311**, pp. 399-436, 1992.

[5] L. Walckiers, *The Harmonic Coil Method,* Proc. CERN Accelerator School on Magnetic Measurement and Alignment, Montreux, Switzerland, March 16-20, 1992, (CERN Report 92-05) pp.138-166.

[6] P. Schmüser, *Magnetic Measurement of the Superconducting HERA Magnets and Analysis of Systematic Errors*, Report DESY HERA-P 92-1. Also in Proc. CERN Accelerator School on Magnetic Measurement and Alignment, March 16-20, 1992, CERN Report 92-05, pp. 240-273.

[7] S. Bidon, J. Billan, F. Fischer and C. Sanz, *New Technique of Fabrication of Search Coil for Magnetic Field Measurement by Harmonic Analysis*, CERN AT-MA Internal Note 95-117, May 1995.

[8] E. Willen, P. Dahl and J. Herrera, *Superconducting Magnets*, in Physics of Particle Accelerators, Vol. 2, M. Month and M. Dienes, eds., AIP Conf. Proc. 153, American Institute of Physics, New York, 1987, pp. 1229-76.

[9] J. Herrera, G. Ganetis, R. Hogue, E. Rogers, P. Wanderer and E. Willen, *Measurement of the Magnetic Field Coefficients of Particle Accelerator Magnets*, Proc. 1989 IEEE Particle Accelerator Conference, March 20-23, 1989, Chicago, IL, IEEE Catalog No. 89CH2669-0, pp. 1774-6.

[10] J. Billan, CERN, private communication.

[11] C.R. Gibbons, D.W. Bliss, R.E. Simon, A.K. Jain and P. Wanderer, *Locating the Magnetic Center of the SSC CDM Using a Temporary Quadrupole Field*, Proc. 1992 Applied Superconductivity Conference, Chicago, IL, USA, August 23-28, 1992.

[12] J. Herrera, *Effect of Sag in Tangential Coil on Multipole Coefficients*, Magnet Test Group Note No. 179, January 20, 1982, Brookhaven National Laboratory, Upton, New York.